1201

NATIONAL ADVISORY COMMITTEE FOR AERONAUTICS

TECHNICAL MEMORANDUM

No. 1201

ROTATION IN FREE FALL OF RECTANGULAR WINGS OF ELONGATED SHAPE

By Paul Dupleich

Translation of "Rotation par Chute Libre des Ailettes Rectangulaires de Forme Allongée." Publications Scientifiques et Techniques du Secrétariat d'État a l'Aviation, No. 176, 1941

NACA

Washington

April 1949

PREFACE

The present report of Mr. Dupleich is the summary of a very extensive experimental study of the well-known mechanical phenomenon: the rotation in free fall (in air, for instance) of more or less elongated rectangles cut out of paper or pasteboard. This phenomenon, the conditions for existence of which depend chiefly on the elongation of the small plate and its weight per unit area, is essentially an aerodynamic phenomenon and as such, raises questions of a certain interest to our department.

The author has applied himself to this study as one would do in the case of a physical phenomenon which analysis has not yet ventured to penetrate and which would require, to begin with, investigation of its general characteristics. Actually, one had to deal here with a problem of mechanics, the active forces of which are, on one hand, the weight of the body, and, on the other, the aerodynamic forces related to the motion. Thus one is justified in thinking that the action of the fluid should have been analyzed in order to determine its mechanism and distribution, for the laws of the motion are only a consequence of this action, and knowledge of these laws is in itself only a partial aspect of the problem.

This problem gives rise to certain fundamental questions to which one would like to see an answer given. Why, for instance, does the plate in its falling motion rotate about itself, thus leading one to assume that, at least under certain conditions, another state of steady fall would not be possible? How is it that under the same conditions the rotation leads to a steady motion, that is, to the existence of a mean equilibrium between the aerodynamic forces and the weights? And how does this same type of steady motion under different conditions become unsteady to give way to other types of fall, now steady, but which would have been impossible under the previous conditions? Subjects like these have only been touched on insufficiently by the author who thought he must limit himself to strictly experimental study.

Thus, at first sight, this report will perhaps appear to the specialists as a work lacking in the spirit of aerodynamics.

We believe to have shown elsewhere - and no doubts seem possible - that the modern concepts of the mechanics of fluids do not have the range attributed to them, that they have not been more than attempts (it is true, often successful in very limited problems), that one has too frequently taken a success as proof, that one has committed the serious scientific error of drawing very general conclusions from a theory verified only under a single one of its aspects and of believing in them, that one has lightly assumed the existence of a grandiose theory where there was only systematic, all too systematic, exploitation of poor mathematical artifices, that, in a word, the modern theoretical mechanics of fluids is not a coherent whole.

NACA TM No. 1201

However, it is certain that it should have penetrated more deeply into the scientific groups concerned, for the services rendered by the preliminary investigations it has promoted are too real to be justifiably ignored, whatever illusions certain aerodynamicists may have entertained about it. And if a physicist, in dealing with an aerodynamic problem, shows that he is not familiar with the modern theories or does not attempt to make use of them, one must have the courage to recognize that this negligence constitutes a gap.

A gap - but let us not deplore it too much, and not be so narrow-minded as to stigmatize it. In fact, too many people tend to believe, once and for all, in the perfection of a theoretical framework and to forget about both observation of facts and their interpretation as not to make it desirable to see appear, from time to time, an essentially experimental study like that of Mr. Dupleich, the merit of which lies precisely in the objectivity of its abundant documentation.

And this is why - in spite of the reservation that had to be expressed - the Ministry of Aviation has seen fit to publish in its collection this report of Mr. Dupleich which owing to its substantial qualities well deserves this mark of honor.

Pierre Vernotte
Chief Engineer of Aeronautics

TABLE OF CONTENTS

NATIONAL ADVISORY COMMITTEE FOR AERONAUTICS

TECHNICAL MEMORANDUM NO. 1201

ROTATION IN FREE FALL OF RECTANGULAR WINGS OF ELONGATED SHAPE*

By Paul Dupleich

HISTORY AND SUMMARY

The free fall of rotating rectangular wings had been considered by Maxwell in 1853 (reference 1). In a very brief theoretical study this author attributed the sustained rotation to the air resistance whose moment, with respect to the center of gravity, maintains the motion and varies periodically with the speed of fall. He also showed that the fall departs from the vertical in a plane normal to the axis of rotation and in a sense depending on the sign of this rotation. He adds that, if the axis is inclined with respect to the horizon, the trajectory is no longer rectilinear but helicoidal, which is inaccurate, because the axis will always straighten out again and assume a horizontal position. Lastly, Maxwell mentions the spiral fall of elongated trapezoids.

In 1881 (reference 2) Mouillard gave a sketchy explanation for the sustained rotating motion of rectangular plates which placed the center of pressure (which he terms "center of gravity") outside the geometrical center; without specifying the conditions of their determination he plotted the trajectories of the vertices of the rectangle with loops of large area, which in reality appears to be only a very exceptional case.

In 1904 (reference 3) H. Moedebec studied the problem of Professor Köppen's rotating parachute (1901), a type of which had been exhibited in Berlin in 1902. At the right and left of the parachute jumper, two sails of 6×19.5 m^2 in over-all dimensions revolve in the manner of rotors with paddles, by autorotation about a horizontal axis, and impose a trajectory, slightly inclined with respect to the horizon, on the system. The apparatus was to be transformed into a flying machine by the addition of a motor which was to have maintained a speed of rotation sufficient to regulate the slope of the trajectory and even to make it ascend at will.

The same question has been envisaged theoretically by Joukowsky (reference 4) in the general framework of autorotation. As application of his fundamental theory on the lift of surfaces, he shows that the

---

*"Rotation par Chute Libre des Ailettes Rectangulaires de Forme Allongée." Publications Scientifiques et Techniques du Secretariat d'État a l'Aviation, No. 176, 1941.

The scale for the wing itself is given in the position 00' (fig. 3), perpendicular to the mean inclined plane, or else by a reference scale of known length placed in the plane of fall.

The time of exposure is inscribed on each negative by the simultaneous photograph of a black revolving disk, a narrow (3°) sector of which is left white. Actuated by electric motor and frequently checked, the speed of the disk is one revolution in 1.44 seconds. The angle of the photographed sector is measured with a Leneveu protractor at close to 2 minutes. The relative error is always less than 0.0001. The lengths at 1/20 millimeter are measured on the enlarged positive or on the negative with a microscope. This accuracy yields a relative error generally less than 0.005.

The characteristics of a wing of negligible thickness are:

chord 2a

span 2b

wing loading Δ

aspect ratio: $k = \frac{b}{a}$

a and b are always expressed in centimeters, and Δ in grams per dm^2.

Platform Launching - Acceleration of Rotation

The wing is placed on the platform P, its long side parallel to the edge O and normal to the plane of figure 1. The center of gravity G, being outside of the support, the gravity effects the launching (fall and rotation) as soon as the operator frees the clamp T. By regulating the inclination of the platform P with respect to the horizon and lever arm $OG = l$, the falling wing is given enough kinetic energy to speed up the incipient rotation and cause the mean trajectory to be directed toward the right of the figure. Assuming zero sliding on edge O of platform P, the released wing revolves like a pendulum about this edge. When it reaches the vertical plane passing through O, the launching, characterized by the speed of rotation reached at this instant, may be considered complete. The calculation of this initial speed of rotation, without interference of the resisting couple of the air, is known to give only an approximate indication, by defining an upper limit that is never reached.

Let m represent the wing mass, I the moment of inertia with respect to the edge of the platform and ω_o, the initial speed of rotation. The kinetic energy theorem gives:

$$\frac{I\omega_o^2}{2} = mgl(1 + \sin\beta)$$

where:

$$I = \frac{m(a^2 + 3l^2)}{3}$$

By putting $\omega_o = 2\pi N_o$ (N_o = revolutions per second)

$$N_o = \frac{1}{2\pi}\sqrt{\frac{6g(1 + \sin\beta)l}{a^2 + 3l^2}}$$

a value independent of the weight and of the span 2b.

To illustrate: the usual initial speed for a series of homogeneous rectangles of the same chord of 3.6 centimeters, launched with $2l = a$, on the horizontal support ($\beta = 0$), is 4.8 revolutions per second.

In these conditions of launching, the initial speed of rotation, generally lower than the speed of steady motion, agrees quite well with experience.

The rotation is accelerated during the fall. A wing launched practically without initial speed $\left(\frac{l}{a} = \text{small}\right)$ quickly assumes a speed of rotation, which increases at the same time as the speed of fall. If the wing is light, the acceleration lasts only for several revolutions, at the end of which the steady motion is practically attained. In the laboratory the acceleration measurement is easier with the relatively heavy rectangles (thick pasteboard), the speed of rotation for a 155 x 15 millimeter wing, weighing 10.9 grams per decimeter^2, launched with $N_o = 6.9$ reaches 48 revolutions per second, after a fall of about 3 meters. A 110 x 15 centimeter plate weighing 550 grams, released on the special platform, with $N_o = 3$, from the top of the 18 meter tower reaches the ground at considerable angular speed (the angle of fall being about 75°). Plates of iron weighing 1 kilogram attain steady motion after a fairly long fall, which can be reduced by reason of an increase of N_o.

Wings of very small dimensions, such as flakes of graphite, can also turn in the air. In all those cases if the launching is appropriate, the steady motion can be realized, giving rise to an infinite motion of descent, as will be shown hereinafter.

CHAPTER II

KINEMATICS OF THE AVERAGE MOTION

In steady motion, with a legitimate approximation formulated later in the analysis, the center of gravity G of the wing MM' describes, at a constant speed V, a straight line XY inclined at an angle α with respect to the horizon (fig. 2). Simultaneously the wing MM' turns at constant speed ω about its major horizontal axis of which G is the trace on the vertical plane which contains XY.

The wing moves as if it were integral with a straight circular cylinder C, of the same axis and of diameter 2a, sliding and counter-rolling along the line of greatest slope of the inclined plane WZ.

The instantaneous speed of point A of the cylinder is the resultant of the rectangular speeds $a\omega$ and V. The instantaneous center of rotation G situated on the normal in G to XY, verifies the relation:

$$CG = AG \cot ACG = \frac{V}{\omega}$$

With v denoting the speed of sliding motion

$$V = v + a\omega$$

Consequently, the base of the motion is the straight line QR, parallel to XY, of the ordinate

$$PC = \frac{-v}{\omega}$$

The roller is the circle of radius $\frac{V}{\omega}$, rolling without sliding on the upper inclined plane.

The wing, of span MM' = 2a, is a fraction of a diameter of this roller; its envelope is identical with the envelope of this diameter, hence the well-known equations (axes of fig. 3, origin O_1)

$$\begin{cases} x_1 = x = \frac{V}{2\omega} (2\varphi - \sin 2\varphi) \\ y_1 = \frac{V}{2\omega} (1 - \cos 2\varphi) \end{cases}$$

The curve O_1AB represents the part corresponding to the spatial period $\frac{\pi V}{\omega}$. The distance O_1B is termed "span of the arch."

The point of contact E, of the diameter, with its envelope is found immediately by plotting the normal to the trace of the wing through C. At instant t this point has minimum speed, ω CE. Moreover, at the subsequent instant the adjacent points of the wing also pass at the same point. In consequence, the photograph of the envelope is very luminous and often alone visible.

To the point of inflection O_1, there corresponds an actual pivoting of the enveloped diameter about one of its ends. But the arcs of the envelope comprised between the parallels qr and QR, which are touched only by the geometric extensions of the wing, do not appear on an exposure at $V > \omega a$, which is the most frequent case, the limit points of real tangency being given by

$$\cos \varphi = \frac{a\omega}{V}.$$

They are most often replaced by connecting arcs which outline the trajectories of the wing tip near the pivoting point O_1. The linear speed of this tip, being thus very small, can produce an image on a plate almost as much as the points of contact with the envelope.

Study of Negatives

Let M_1M_2 and $M'_1M'_2$ represent the positions of MM' at the start and finish of a photographic exposure. They still correspond to the tangents to the two tips of the envelope arc fixed on the negative; hence the rotation $(\varphi_2 - \varphi_1)$ during the time Δt read on the chronograph.

A mean speed of rotation is deduced. The true angular velocity is periodic. Consequently, in view of the evaluation in fractions of revolutions, the mean speed thus computed is not absolutely equal to the mean speed over a period, especially for the short and slow falls, but the large number of negatives obtained assure sufficient accuracy, since the operation is always extended over several periods of the phenomenon. More rigorous values will be deduced later from the experimental study of the rotation.

The corresponding positions G_1 and G_2 of the center of the section are given by the centers of $M_1M'_1$ and $M_2M'_2$ or else by the extreme positions of the luminous index mark.

A mean speed V is thus defined. The remarks made concerning ω remain in force, V being actually periodic.

Quantity $\frac{V}{a\omega}$ is given either starting from V and from ω, or by $\frac{D}{2\pi na}$, where D is the distance traversed by G during several revolutions n, measured along with a directly on the photograph.

The tangent common to the arcs of the roller or the envelope defines the angle α (fig. 2).

The measurement without correction of α requires a fall parallel to the screen. Moreover, this measurement may be falsified by accidental rolling and yawing motions of the wing. Having a sufficient number of negatives of the same wing available, only those most nearly correct were utilized. The photograph (fig. 4) represents the trajectory of the 12×2 centimeter^2 wing for which $\Delta = 1.3$ grams per decimeter^2.

CHAPTER III

SUSTENTION OF STEADY MOTION OF FALL

Let axis Ox be represented (fig. 5) by the tangent common to the arches of the envelope, inclined at angle α to the horizontal, O coinciding with a contact point; axis Oy is perpendicular. The directions are positive downward. Let x and y denote the coordinates of the center of gravity G, i the angle of incidence which Ox forms with the half-wing whose edge shifts in the sense of the relative wind, counted positive starting from Ox in the direction of the rotation; i varies periodically from 0° to 180°.

With R as the air resistance (resultant of aerodynamic forces), as function of i, the moment of this force R is decomposed, with respect to the large axis of symmetry of the wing, into Γ, the "static" moment, which will be the real moment of the aerodynamic forces if incidence i was constant, and into γ, a supplementary couple due to the wing rotation. Lastly, let I be the moment of inertia of the wing with respect to the preceding axis.

The air resistance R is assumed normal to the plate at every instant. In reality, of course, the direction of the air thrust slopes at a greater or lesser angle from one side or the other of the normal, depending on the incidence of the plate. So in the equations the resistance is introduced as being active only in the rotation. The tangential component is involved in the forward motion of the plate.

The equations of motion in the foregoing conditions read:

$$\begin{aligned} x'' &= mg \sin \alpha - R \sin i \\ y'' &= mg \cos \alpha - R \cos i \end{aligned} \tag{1}$$

$$I \frac{d^2 i}{dt^2} = \Gamma + \gamma \tag{2}$$

These equations themselves disclose that the motion of G like the motion about G cannot be strictly uniform. But experience indicates that they are quite often very approximately uniform, the periodic variations of the speeds being of low amplitude.

Therefore

$$mg \sin \alpha = \frac{1}{\pi} \int_0^{\pi} R \sin i \, di = P$$

$$mg \cos \alpha = \frac{1}{\pi} \int_0^{\pi} R \cos i \, di = Q$$

according to which angle α satisfies the relation

$$\tan \alpha = \frac{\int_0^{\pi} R \sin i \, di}{\int_0^{\pi} R \cos i \, di} \tag{3}$$

The explanation is based on the inertia of the steady motions, the principle of which is known, but needs further study, since the two terms have been little associated up to now.

The variations of R sin i and R cos i between 0° and 180° can be represented by the curves of figure 6a, which consist of two unconnected branches, corresponding to two different aerodynamic conditions. Of the two values which give the curves for R cos i on abscissa $i = 30^\circ$, for example, nothing defines beforehand that which should be retained in a concrete case.

In the static conditions (i constant) to which the preceding curves refer, sudden jumps occur from one curve to another (from one steady motion to another) for no apparent reason. The mechanism of this indecision of the steady motion or of its instability is still too little known.

In the dynamic conditions, that is, those of the motion in question, the aerodynamic conditions are entirely different. Around the rotating wing there are turbulent circulations, the whole of which represents a complex phenomenon, but which unquestionably seem to belong also to two different conditions, separated, as in the static conditions, by a real discontinuity in the neighborhood of the angle $i = 30^{\circ}$. This discontinuity is represented by the vertical jump AC on the R cos i curve in figure 6b. The passage from A to C, i being assumed increasing, demands substantially less action than in the static conditions; the instability of the condition OA is reduced; the existing steady motion tends to be prolonged as much as possible; it is in some manner endowed with inertia.

Figure 7 shows the variations of the couples Γ and γ plotted against i. The integral $\int_0^{\pi} \Gamma \, di$ has a positive value; it represents the motive energy of couple Γ during the half revolution. The curve MNP of couple γ is very flat; the maximum and minimum have fairly close values. Evidently

$$\int_0^{\pi} (\Gamma + \gamma) \, di = 0$$

The motive energy of Γ, which is represented by the shaded area in figure 7, is absorbed, in steady motion, by the resisting energy of couple γ.

The total couple $\Gamma + \gamma$ cancels out for $i = \beta_1$ and $i = \beta_2$ (figure 7). In the interval $\beta_1 < i < \beta_2$, the aerodynamic couple is motive, for the rest of the period, resisting. In the motive interval, the wing must therefore store up enough kinetic energy to clear the second interval. Consequently, the motion cannot be sustained unless the moment of inertia of the plate is sufficiently high; otherwise the rotation stops in a position of the wing beginning at which the latter starts to slide. This explains why the light rectangles of large area and aspect ratio k near 1, whose steady motion is very slow, turn irregularly or not at all. The stable rotation of such rectangles is always obtained by reducing the chord.

The resistance R, on assuming the speed V of the center of gravity constant, is approximated at

$$R = K_1 SV^2,$$

where $S = 4ab$ is the wing area; K_1 a coefficient as function of i and depending upon the aspect ratio $k = \frac{b}{a}$ of the wing. Consequently

$$R \sin i = K_1 \sin i \, SV^2$$

and on putting

$$K = \frac{1}{\pi} \int_0^{\pi} K_1 \sin i \, di,$$

the formula

$$mg \sin \alpha = KSV^2$$

or

$$\Delta \sin \alpha = KV^2$$

according to which V is proportional to $\sqrt{\Delta}$. This law has been verified by experience.

The mean value in a quadrant ($0 < i < 90^\circ$ or $90^\circ < i < 180^\circ$) of the component R cos i (lift) is proportional to the corresponding area of the curve R cos i plotted against i (fig. 6). This area is larger, in absolute measure, for the first quadrant than for the second, in spite of the geometric symmetry existing between the two quadrants; if the continued variation of incidence i had no effect on the distribution of the aerodynamic forces, the mean values of R cos i in the two quadrants are equal and of opposite sign. The mean lift in the complete period is zero and therefore cannot be opposed to the weight component mg cos α during the steady motion of the wing. Hence the existence of a mean thrust at right angles to the inclined trajectory of the wing.

This conclusion, which can be explained by the phenomenon of aerodynamic inertia, seems to be in agreement with the general relation between lift and circulation, which constitutes Joukowsky's theory (reference 4, p. 54). On admitting, in fact, that the rotation of the wing sustains by inertia a mean circulation (C) having the direction of this rotation, (fig. 8), there must correspond to this circulation a lift Q which is directed upward, considering the direction of the relative speed V.

Inertia of Steady Rotatory Motions and Resonance

The inertia of steady motions is a principle, the justification of which is found in the closely connected explanation furnished by a large number of phenomena. Is it possible to obtain a direct check on it in the case of the aerodynamic resistance for a variable incidence?

To be successful in a static test the incidence variations must, undoubtedly, be more rapid than those obtainable by stopping the variation for measuring the effect before producing a new one. While this may be applicable to rubber under variable tension, it is far from being the same when aerodynamic actions, such as come into play in the phenomena in question, are involved. Born of circulation and vortices which attain their full development in an extremely short time interval, these actions must be measured at the same instant the phenomenon of discontinuity involved is reached and this situation must be encompassed by measurements immediately before and after in the process of evolution.

The conditions required are therefore practically unattainable. Even in the case where a record of the phenomenon is possible, it is never certain that the results agree with reality; having obtained a large number of graphs representing the studied variation, an average must be made, which is always of doubtful interpretation.

The phenomena of resonance, easily obtainable for periodic variations, produce these averages automatically. In autorotation, in a uniform wind, a wing can transmit the variations of periodic efforts which it experiences to an oscillating dynamometer; degrees of freedom may be prescribed for the dynamometer in proportion to the forces, and the maximum and minimum values identified.

The air current being vertical, the wing is made to rotate about its large horizontal axis, by means of two pins supported on two cup bearings on a horizontal rectangular frame (fig. 9). Soldered to the frame, perpendicular to its plane, is a narrow metal sheet whose axis extends the line of the bearings of the frame. At its other end, the sheet is clamped in a solid support; the system is thus able to oscillate in the horizontal plane by elastic bending.

In the absence of rotation, the action of the wind does not give rise to oscillation; in steady autorotating motion, the vertical components of the instantaneous resistances have no effect on the motion of the system, which can be produced only by the variations of the horizontal component (normal to the wind) of the aerodynamic resultant.

But, as it is, the system is too sensitive to give acceptable results. Without a damping device it may, with 12 centimeters seating, produce amplitudes of from 5 to 10 millimeters, which disturb the autorotation considerably to the point of complete cessation. This can be remedied by damping; by means of two 2-centimeter^2 vertical paddles dipped in glycerin. This affords a sufficiently stable steady motion where only the resonance amplitude, less than a millimeter, is perceptible in the stroboscopic sight.

With a 30×40 millimeter^2 wing, rotating at a speed of 6.7 revolutions per second in a uniform air flow of 3 to 4 meters per second (introduced by a vertical pipe of 70-millimeter diameter, the orifice being 50 millimeters below the frame), the maximum effort for increasing incidences was found at an incidence of about 25°. This result in correlation with others was obtained by a different experimental method.

CHAPTER IV

EXPERIMENTAL DETERMINATION OF THE ELEMENTS OF STEADY MOTION

To a given wing there corresponds a given steady motion, defined by its three parameters α, $\frac{\omega}{2\pi} = N$, and V. The experimental study must furnish these three parameters in form of three more or less complex functions of a, k, and Δ. The curves of figures 10 to 13 represent these functions.

The thickness 2c of the wings, which is assumed negligible compared to the other two dimensions, does not enter in these formulas. This assumption is perfectly legitimate for the light paper; thus, the thickness of the lightest paper utilized ($\Delta = 0.14$ gram per decimeter^2) is equal to 0.005 centimeter for a span of 1.5 centimeters, which corresponds to $\frac{c}{a} = 0.003$. For the large size wings, made of pasteboard to insure rigidity, the thickness reached 0.3 centimeter for a span of 32 centimeters, or approximately $\frac{c}{a} = 0.01$.

The amplitude of variation of the parameters is necessarily very limited. If k is too close to unity, certain wings turn badly or not at all, simply oscillating about a mean horizontal position. Nevertheless, it was possible to effect measurements for $k < 1$, over the several half-revolutions of a fall which is not sustained because it is unstable. The test points obtained this way are located on a curve extending the curves of figures 10 to 13 where they are recorded.

If k exceeds an upper limit, the wings bend. This limit, which increases with the thickness, is rather high for the pasteboards which are also very heavy, and which, besides, are difficult to put in steady motion at the height of fall permitted by the limits of the laboratory. The bending is eliminated by fixing on each face of the wing, normal to its plane and along the major axis of symmetry, a narrow strip of paper folded square, but then the additional resistance introduced modifies the phenomenon (in particular, it increases angle α).

A special chapter is devoted to this particular case, where the bending of the wing assumes real importance. The values of wing loading Δ for which it was possible to obtain complete measurements at the height of fall available, range between 0.14 (cigarette paper) and 13.1 grams per decimeter^2.

Table I gives the test data of which only a few are reproduced in figures 10 to 13; E, F, and H represent the three functions of α, N, and V which define the steady motion for a given wing.

The quantities

$$E = (2ak^3)^{1/4} \tan \alpha$$

$$F = 2a^{3/4} k^{-1/3} N$$

$$H = 10^{-3} (2a)^{\mu} \frac{V^2}{\sin \alpha}$$

are approximately constants for a given value of Δ (last column of table I); μ is a coefficient as function of Δ represented by the formula

$$\mu = 0.27\, \Delta^{-1/3} \text{ (see fig. 14)} \qquad (1)$$

As functions of Δ, quantities E, F, and H vary along the curves of figures 15, 16, and 17, which correspond to the following equations (a in centimeters, Δ in grams per decimeter^2):

$$\left.\begin{aligned} (2ak^3)^{1/4}\, \Delta^{-1/5} \tan \alpha &= 2.7 \\ (2a)^{3/4} k^{-1/3} N &= 1.8\, \Delta + 9.5 \\ 10^{-3} (2a)^{\mu} \frac{V^2}{\sin \alpha} &= 23\, \Delta + \epsilon \end{aligned}\right\} \qquad (2)$$

These relations define the values of the steady motion within the limits of the zone where the parameters a, k, Δ can be practically realized.

Quantity F cannot be less than 9.5, which forms the lower limit of N for any given values of a and k.

Quantity H is represented as a function of Δ by a straight line which does not pass rigorously through the origin; but ϵ is negligible for the usual values of Δ; the third equation of (2) becomes then

$$10^{-3}(2a)^{\mu}\frac{V^2}{\sin\alpha} = 23\Delta$$

hence, with S designating the area of the wing,

$$\Delta S \sin\alpha = mg \sin\alpha = \frac{10^{-3}}{23}(2a)^{\mu} SV^2 = KSV^2$$

The coefficient $K = 43.5 \times 10^{-6}(2a)^{\mu}$ (a in centimeters) is to be compared to the coefficient of resistance of a plate normal to the wind.

Through the medium of μ (equation (1)), K is dependent on a and Δ. For high values of Δ the factor $(2a)^{\mu}$ tends toward unity, when the law $\mu = 0.27\Delta^{-1/3}$ is extended. The mean resistance to the translation follows then the law $43.5 \times 10^{-6} SV^2$. The wing, whose rate of rotation is then considerable, can be likened to a cylinder with a maximum cross section S; the coefficient of resistance is, in fact, near the coefficient of the cylinder (reference 6).

The elimination of α between E and H leaves

$$\sin^2\alpha = \frac{E^2}{(2ak^3)^{1/2} + E^2}$$

hence

$$V^4 = 10^6 \frac{H^2 E^2}{(2a)^{2\mu}\left[(2ak^3)^{1/2} + E^2\right]}$$

or, written explicitly according to equation (2)

$$V^4 = 3856 \times 10^6 \frac{\Delta^{12/5}}{(2a)^{2\mu}\left[(2ak^3)^{1/2} + 7.29\,\Delta^{2/5}\right]} \qquad (3)$$

V is given in centimeters per second by this formula.

The experimental curves (fig. 12) give as function of k, for 2a and Δ constant, a hyperbolic variation of V in accord with equation (3).

The formula giving the ratio $\frac{V}{aN}$ is more complicated. For the values of this ratio below 6.28, the roller paths of the vertices of the wing are looped. But it is difficult to obtain such trajectories, since bending is most often an obstacle to their formation. (For this reason the curves of figure 13 are found limited.) However, their existence has been proved with wings corresponding to $\Delta = 4.8$ grams per decimeter^2, $2b = 100$ centimeters, and $2a = 20$ and 31 centimeters, giving $\frac{V}{aN} = 5.7$.

To study the variation of V with b constant, 2a in (3) is replaced by $\frac{2b}{k}$, so that

$$V^4 = 3850 \times 10^6 \frac{\Delta^{12/5} k^{2\mu}}{(2b)^{2\mu}[(2b)^{1/2}k + 7.29\Delta^{2/5}]} \qquad (4)$$

If Δ is constant, V^4 varies as

$$Z = \frac{k^{2\mu}}{(2b)^{1/2}k + E^2}$$

where E^2 replaces $7.29\Delta^{2/5}$. The derivative

$$Z' = \frac{k^{2\mu-1}\left[2\mu E^2 + 2b^{1/2}k\,(2\mu - 1)\right]}{(2b^{1/2}k + E^2)^2}$$

cancels out for the two values of k:

$$k' = 0$$

$$k'' = \frac{2\mu E^2}{2b^{1/2}(1 - 2\mu)}$$

For very small values of Δ, formula (4) lacks accuracy. For $\Delta = 0.14$, in particular, the value of V computed by means of the expression H is too low. The coefficient μ computed by formula (1) must be replaced by $\mu' < \mu$. This gives, within the present experimental limitations: $1 - 2\mu > 0$, even for $\Delta = 0.14$, whereas the curve of figure 14 gives $1 - 2\mu = 0$.

Quantity V presents a maximum for $k = k''$. For $\Delta = 1.3$ and $2b = 12$, $k'' = 2.3$. Table II, established experimentally to evidence

this maximum, affords an interesting verification of the formulas. From the existence of this maximum, the explanation of an unusual singularity of motion is deduced in chapter XIII.

The contents of table II were used to plot the curve ($\Delta = 1.3$, $2b = 12$) of figure 12; it represents a maximum for $k = 2.3$.

The expressions

$$\tan \alpha = \frac{E}{(2b)^{\frac{1}{4}} k^{\frac{1}{2}}}$$

and

$$N = \frac{F k^{\frac{13}{12}}}{(2b)^{\frac{3}{4}}}$$

indicate that α decreases and N increases for Δ and $2b$ constant.

For the same values of k and Δ, that is, for similar rectangles having the same wing loading, the constants of the steady motion vary with the dimensions of the rectangle. These variations are illustrated by the four curves in figure 18.

CHAPTER V

ACTUAL MOTION OF THE CENTER OF GRAVITY

1. Trajectory

According to equations (1) (chapter III) the movement of the center of gravity cannot be rectilinear and uniform. It is studied by photographing its trajectory, the outline of which coincides with that of the center of the small side of the wing, obtained by a white round index mark. The wing is slightly blackened so that the envelope still remains visible on the negative.

The trajectory of G in all photographs, oscillates to both sides of Ox. These oscillations are not attributable to launching, since they are well developed from the start. In fact, as soon as the steady motion of fall is reached, they themselves are periodic, the period being of a

half-revolution; after several meters of vertical fall no damping is observed. The assumption of disturbed trajectory is equally inapplicable, because the period of the disturbed oscillations is different from a half-revolution; besides, such oscillations are damped.

The motion of G comprises thus an oscillation to both sides of Ox parallel to Oy. The nonsinusoidal oscillation is unsymmetrical with respect to the position O_1A of the wing, corresponding to $i = 90^\circ$ (fig. 5). The trajectory meets this straight line O_1A at point G_0, of the negative ordinate y_0, which is not a minimum (maximum in absolute value); it is considerably incurved up to point G_1 of ordinate y_1 (minimum of y) and becomes tangent to the envelope in point G_2, very far upward toward the lower vertex O' of the arch. From this point of contact, G_2 on the curve is very flat on the envelope; generally, for low values of V the part practically common to the two curves ceases near O'; for high speeds V it may extend beyond O'. In all cases the maximum ordinate y'_1 (positive) of the oscillation (point G') is near zero or null.

Owing to the oscillation, the position O_3D of the wing, for which the true angle of attack is equal to 90°, is set with respect to O_1A in the direction of motion.

The oscillation, quite considerable for rectangles of large span and whose fall and rotation are slow, is slightly perceptible on the trajectory of the small rectangles in rapid motion.

The displacement of the point of contact over the length of branch O_1G_2 is equal to a. The motion of the wing with respect to its envelope is then very nearly a pure rolling motion (minimum sliding). From G_2 up to O' (trajectory practically identical with the envelope), the sliding motion increases; it is still considerable on the remaining branch $O'G_2$ of the arch.

The difference in incidence i, between the two wing positions corresponding to a maximum and minimum oscillation, is around 90°; i being equal to $90 + \beta$ at minimum G_1, the approximate equation of the trajectory is of the form

$$y = \epsilon_1 + \epsilon_2 \cos 2 (i - \beta)$$

where ϵ_1 and ϵ_2 are defined by the relations

$$\epsilon_1 + \epsilon_2 = y'_1$$

$$\epsilon_1 - \epsilon_2 = y_1$$

The value of $90^\circ + \beta$ is, moreover, poorly defined, since a relative minimum is involved.

2. Speed

A rather narrow strip of paper is glued to front and rear section of the wing (blackened pasteboard) so that the motion is not modified. The light source is an electric arc, fed by 50-cycle a-c giving a maximum luminous intensity 100 times per second. To each maximum flash corresponds one instantaneous view of the section. The trajectory of G is projected on the space in the middle of the straight successive images of the section. It can also be obtained with a black center.

The successive positions cut this trajectory in segments in one-tenth of a second, the length of which estimates the instantaneous speeds.

The accuracy is satisfactory if, before measuring, the spaces of maximum luminous impression which correspond to the equidistant exposures are outlined on the negative.

It seems simpler to photograph the path of the index mark placed in the center and illuminated alone, by electric arc, but this would require a powerful illumination. The first method has the advantage of locating the successive positions of the wing which then permit the variations of ω to be determined.

The minimum speed V_1 of G is largely found in G_1 (minimum of y), while the maximum largely corresponds to the maximum of sliding motion.

The minimum speed is compared to the previously defined mean forward speed V. The corresponding variation $\frac{V - V_1}{V}$ is considerable for large size rectangles; table III shows various values along with the corresponding values of y_o, y_1, and β.

From the equation

$$x'' = mg \sin \alpha - R \sin i$$

it follows that x' increases for $i = 0$, x'' being positive. For $i = 90^\circ$, $R \sin i$ is approximately maximum. Since its mean value is equal to $mg \sin \alpha$, the maximum is higher than this value; consequently, x'' is then negative, x' passes through a maximum in the interval. For $i = 180^\circ$ x'' is positive, x' passes through a minimum in the part of the trajectory corresponding to $G_1 0'$.

If the tangential component of the resistance R, disregarded in the foregoing, is introduced, the results show that the latter favors the advance for incidences ranging between around 20° and 160°, that is, for a large portion of the trajectory located entirely above the plane tangent to the envelope arches; for the rest of the period, on the other hand, the effect is a resistance to the advance.

3. Angular Speed

The equation

$$I \frac{d\omega}{dt} = \Gamma + \gamma$$

defines the variation of the instantaneous angular speed, controllable on the photograph of the successive positions of the wing section, at 0.01-second intervals.

For symmetrical positions with respect to $O_1 A$ (fig. 5) the successive images of the tip are spaced farther apart on the arc $0 0_1$ of the envelope than on arc $O_1 0'$. The angular speed ω increases along arc $0 0_1$ and passes through a maximum at $i = \beta_2$. As for the minimum located near $i = 0$, it cannot be identified very accurately on the photographs.

With N_2 signifying the maximum speed in revolutions per second, N the mean speed defined by chronograph, Ω the angle of rotation described in 0.02 s, table IV gives the results of the effected measurements.

Quantity Γ cancels out approximately for $i = 0$ and $i = 90^\circ$. Since γ is consistently negative, the total couple for these two values of i is negative, for which ω is decreasing. Quantity Γ reaches its maximum for a value of i comprised between 0 and 90°; $(\Gamma + \gamma)$, zero for one revolution on the average, is then positive,

and ω increases. In consequence, $(\Gamma + \gamma)$ cancels out for $i = \beta_1$ and β_2 $(\beta_1 < \beta_2)$, the angles between 0° and 90°, to which the minimum and maximum of ω correspond.

In reality, Γ is not canceled for the position O_1A but for O_3D; this divergence slightly shifts the maximum of ω toward O_2B.

An approximate expression of ω reads

$$\omega = \Omega_1 + \left(\sin 2i + \frac{1}{2} \sin 4i\right)\Omega_2$$

according to which ω is minimum or maximum for

$$\cos 2i = \frac{-1 \pm 3}{4}$$

To $\cos 2i = -1$ corresponds an inflection of the curve of variation.

The minimum and maximum of ω, which occur, according to the above conditions, for $i = \pm 30^\circ$, are 60° distant, which is not very much different from the obtained results.

Quantities Ω_1 and Ω_2 are determined by writing that the minimum ω_1 and the maximum ω_2 occur for the indicated values, which gives

$$\Omega_1 = \frac{1}{2} (\omega_1 + \omega_2)$$

$$\Omega_2 = \frac{2}{3\sqrt{3}} (\omega_2 - \omega_1)$$

But to place the minimum and maximum at suitable values of i, it is necessary to shift the curve $60^\circ + 2\beta_1$; hence the expression for ω reads

$$\omega = \frac{1}{2} (\omega_1 + \omega_2) + \frac{2}{3\sqrt{3}} (\omega_2 - \omega_1) \left[\sin 2 (i - 30^\circ - \beta_1) + \frac{1}{2} \sin 4 (i - 30^\circ - \beta_1)\right]$$

Figure 20 refers to a wing of 37.5×15 centimeters^2, weighing 9.8 grams per decimeter^2; the steady motion corresponds to

$\alpha = 47^{\circ} 15'$

$N = 4.7$ revolutions per sec

$N_1 = 5.1$ revolutions per sec

$V = 351$ cm/sec

The Enveloping Curve

The periodic variation of V and ω, assumed constant in chapter II along with the oscillation of the path of the center of gravity, must, in reality, divert the form of the envelope from that of the cycloid. The real arcs cannot be symmetrical with respect to O_1A (fig. 5), since different quotients $\frac{V}{2\omega}$ correspond to the two angularly equidistant positions of the wing, the quotients which define the curvature radius of the envelope. In that part of the envelope substantially identical with the path of G, the mean curvature is much less than in that of the corresponding part upstream from O_1A (fig. 21). This asymmetry, which is appreciable for the large-size wings, at slow rotation and forward speed, shifts the point of the envelope, where the tangent plane is parallel to the mean inclined plane, toward downstream. The fact is plainly indicated on the 60×32 centimeter wing, of 6.61 grams per decimeter^2 weight.

CHAPTER VI

RAPID ROTATIONS

The heavy, long rectangles attain considerable speed of rotation during falling. Since the height of fall within the confines of the laboratory is insufficient, the recorded mean values are not, in general, steady motion values. This drawback is evidenced by the fact that in the vicinity of the floor the trajectory is still concave upward and that N still increases. The speed of rotation, comparatively low at start, increases very rapidly. The contour of the envelopes indicates that it has no loops.

With N_0 and H denoting the initial speed of rotation and the height of launching above the floor, N the mean speed of rotation between the approximate height levels H_1 and H_2, table V gives the recorded data. The wings were of heavy pasteboard, did not bend, but their thickness, compared to the chord, was not negligible.

The speed of rotation is, at the bottom of the trajectory, sufficient to produce an audible sound; but it is difficult to derive a measuring procedure from the angular speed of the wing.

Hence the application of the stroboscopic method and the use of the alternating arc. The procedure has proved to be very accurate. Its operating principle is as follows:

The fall being almost vertical at start, the photographic lens is placed at a distance, obliquely with respect to the plane of fall, in such a way as to make the strip of the negative impressed by the moving wing almost vertical. The photograph (positive) appears in form of horizontal, white bands of slightly varying width, unevenly spaced, each corresponding to the lighting received by the wing at the instant of maximum light; black covers the position occupied by the wing when it is in profile view at the instant of maximum.

By way of illustration, assume that N is slightly higher than 50. A black mark is made which corresponds, by assumption, to one position of the profile; 0.01 second later the wing has turned at a half-revolution + ϵ_1, and its actual position corresponds to the first image, which is a very narrow, white, horizontal band. On the second image, the wing will have likewise made a half-revolution + ϵ_2 starting from the first image, hence a little wider band. On each image the wing will have made a half-revolution plus a fraction of a revolution, beginning from the preceding image. When $\epsilon_1 + \epsilon_2 + \ldots + \epsilon_p \sim 1/4$ revolution is reached, the wing, viewed exactly from the front and with maximum lighting, will be stereotyped as a rectangle of maximum width. For $\epsilon_1 + \epsilon_2 + \ldots + \epsilon_n \sim 1/2$ revolution the wing appears substantially parallel to the position corresponding to the first black, hence a second black. Between the two consecutive blacks, the wing has made (n + 1) half-revolutions, within a time interval equal to 0.01 n second. The mean speed of rotation in this time interval is given in revolutions per second by

$$N = 50 \frac{n + 1}{n}$$

Quantity N' and n' denoting the values corresponding to the subsequent luminous region, the ratio of the successively recorded speeds of rotation is expressed by

$$\frac{N}{N'} = \frac{n + 1}{n' + 1} \frac{n'}{n}$$

The same principle of determination applies to the case where $N < 50$.

But the order of magnitude of the mean angular speed which is not arbitrary must be known beforehand. The extension of the method, where N approaches a multiple or submultiple of 50, is easily made. The condition of luminous beats is almost realized on the 155 x 15 millimeter wing. The results are included in table V.

This alternating arc method gives serviceable records even when the foregoing conditions (N near to current frequency, or a multiple or submultiple of the latter) are not realized. After sufficiently accelerated rotation, the envelope becomes discernible on the photographs. It is thus frequently possible to locate the positions in which the flash has impressed the wing on its envelope. The recording of several successive positions permits the approximate determination of the speed of rotation of the wing in its passage to the mean levels of these positions, and to deduce the progressive values of acceleration up to where the steady motion is reached.

The chronograph, photographed simultaneously with the wing, gives an over-all check of the fall. The analysis of a negative with alternating arc is, moreover, facilitated by the comparison of an exposed negative, the conditions of fall being identical. The photograph (fig. 22) refers to the 210 x 25 millimeter wing in table V. The upper height level of the recorded fall is about 20 centimeters of that of launching, the initial speed of rotation being 3 revolutions per second. The two successive half-revolutions, corresponding to the second and third luminous region, fully visible on the photograph, are traversed in 0.09 and 0.06 second, respectively, hence at a mean angular speed of 5.6 and 8.3 revolutions per second. The 2.7 increase in a half-revolution corresponds to a substantial acceleration. The total time of fall, deduced from the total number of images inclusive of those missing, is 0.28 second, the exact time checked by the chronograph.

CHAPTER VII

LAUNCHING

1. Platform Launching

The particulars of the launching from the platform, detailed in chapter I, are as follows:

At a specific inclination β and lever arm $OG = l$, (fig. 23) the initial rotation, which has its inception in the tendency to draw the wing toward the back of the support (toward the right on fig. 23), may become null in an azimuth β' (position 2 in fig. 23), starting at

which the wing slides forward. Without changing the inclination β, but by reducing the lever arm l, which at the same time reduces its resistance R and its moment with respect to O, it is generally possible to permit the rotation to continue resulting in the previously studied steady motion of fall. But the rotation can still be stopped in position 3, by giving rise to a slide, this time toward the rear.

Whether forward or backward, those sliding motions are always of limited distance, at the end of which, for any cause, a rotation begins, which is accelerated very quickly at the expense of the speed of the center of gravity, and which, with a suitable speed of fall, may be sufficient to result in the steady motion that is known. If not, it results in a so-called switchback, which Mouillard undoubtedly wanted to represent in one of his graphs, where the trajectory of the center of gravity is represented with the same curved arches obtained for the envelopes of the wing.

2. Launching by Motor

Two flexible wires (fig. 24b), the ends of which are wound around the ends of the large axis XX', extended from wing A, and anchored by means of a short radial pin, and pass over two fixed pulleys R and are stretched at the other end by two equal weights P. These weights hold the axis against angle plates C which act as bushings. A lever L immobilizes the wing at the start and is released by means of wire F which allows the wing to turn in its bushings up to the instant when the wires become unhooked and the wing drops freely (toward the left in the figure, if the wire is wound appropriately).

A few turns of the wire, with weights of several hundreds of grams are sufficient to give the wing a much higher initial speed of rotation than that of the steady motion. If the speed of rotation has become constant before the wire is released, the driving couple, equal to $2P \times 0.3$ gram per centimeter (0.3 centimeter is the radius of the axis) is equalized by the resisting couple due to the air and to the friction of the axis on the angle plates C. As soon as the weights are released, the resisting couple and the reactions of the supports cease suddenly to be equalized; the result is an abrupt decrease in the speed of rotation. The initial trajectory of G, the slope of which in the origin is that of the resultant T' (fig. 24a), is concave downward. The initial motion is largely parabolic, so much more curved as the rectangles are heavier and the rotation slower. The lighting of the white section of the wing, blackened over the rest of the surface, is secured by the alternating arc. The angular speed N_0 is readily obtained by measuring the angular distance of two successive images.

The following results were obtained:

Rectangle: 33.5 x 19 centimeters

Characteristics: total weight: 50.50 grams; $\alpha = 52^{\circ}5'$;
N = 3.0 revolutions per second; V = 3.28 centimeters per second

The sliding motion being negative at start, according to the present convention, a particularly clear loop is formed, the area of which increases with the launching couple, but afterward vanished quickly. With a 600 gram per centimeter couple, it lasts no longer than the second half-revolution. Here also the trajectory of G (black index mark on white section) is periodically undulated, the mean trajectory presenting an inflection point which is so much lower as the launching couple is greater.

Figure 25 shows the mean trajectories immediately following the launching for the three motor couples given in table VI. There is no sign of any incipient stability oscillations of which Joukouwsky determined the conditions of existence, although the launching by motor with $N_0 > N$ seems to be the mode most likely to produce them, if admitting that they could be produced.

Table VI gives the test data at height level H, measured downward starting from the horizontal of launching. This table shows that N passes through a minimum lower than the speed of steady motion, while N_0 is considerably higher. The initial rotation cannot be maintained and dies down very quickly. The translation following the start is, in fact, insufficient to produce an average motor couple Γ capable of equalizing the resisting couple γ of the air, according to the present theory. By equation

$$I \frac{d\omega}{dt} = \Gamma + \gamma$$

$(\Gamma + \gamma)$ is negative immediately after launching, and consequently ω decreases; but, the motion of translation being accelerated under the action of the gravity, Γ increases and $(\Gamma + \gamma)$ decreases in absolute value; γ varying in the same sense as ω, $\Gamma + \gamma$ are nullified; ω then passes through its minimum. At this instant, the steady motion not being reached, Γ continues to increase; the total couple becomes a driving couple, ω increases, and, consequently, γ also, up to the moment where the speed of translation and of rotation become such that the mean value of $\Gamma + \gamma$ in a half-revolution becomes zero; the wing is then in steady motion.

The curves $N = f(H)$ of figure 26 take the foregoing facts into consideration. It is seen that N reaches its mean value of steady motion without oscillations.

The minimum angular speed increases with the launching couple. For very high initial speed, it may be conceded that N reaches the steady motion by constantly decreasing higher values.

The closely approximated values of table VI indicate that $\frac{V}{aN}$ increases from the start and for the first two values of the driving couple, passes through a higher maximum than at steady motion.

Rectangle: 8.5 x 34 centimeters

Steady motion characteristics: total weight: 33.5 grams; $\alpha = 40°45'$; N = 9.5 revolutions per second; V = 376 centimeters per second

With a 300 gram per centimeter launching couple, the initial speed of rotation is higher than the speed of steady motion. It affords at start four loops, the area of which decreases from the first to the fourth. Again N decreases very quickly and passes through a minimum below that of the steady motion. The results of the measurements are given in table VII.

The mean path of the center of gravity for an identical launching couple is shifted considerably upward with respect to the trajectory of the preceding rectangle. The uneven weights are not the sole cause of this difference; a difference remains even if the lighter of the two wings is symmetrically overloaded so as to equalize the weights. The translation subsequent to launching develops a mean lift Q which is particularly important in the second case, where the initial rotation is greater than in the first case. The effect of this lift is to deflect the path of the center of gravity above the direction T' (fig. 24). Herein may be found a simple justification of Köppen's idea, which, by increasing the speed of rotation of his parachute by adding a motor, should, at the same time, reduce the slope of the path with respect to the horizon, or render it even ascending.

3. Hand Launching

(a) Conventional method.- Mouillard spoke of launching by hand but failed to give an analysis. To be successful would require heavy, elongated rectangles. Grasped by the long sides between thumb and the first two fingers of the right hand, which is moved downward and backward, the wing is thrown vigorously forward and upward, say, at a 45° angle, for example (point 0, in fig. 28); it should be given a high speed of rotation about its large axis held horizontal at the moment of launching. The trajectory, ascending at first, has the form of an incompletely closed loop reminiscent of that of a boomerang (fig. 28).

The initial speed of rotation being such as to direct the mean lift Q downward (Joukowsky law), the result is that the trajectory curves downward much more quickly than it would in the absence of this effect of rotation. Beyond the apex H of the trajectory, the motion continues practically as if it had been launched from a platform in H. Starting at the most forward point I, the gravity is opposed to the lift Q and accelerates the rotation, slowed down by the ascent, to the speed of steady motion.

(b) Other mode of launching.- The method of launching described and analyzed in the following has not been mentioned elsewhere.

Suppose the sense of the initial rotation is changed, that is, from bottom to top for the forward wing half (fig. 29). For this purpose the wing is held between thumb and fingers of the right hand as before, the hand raised above and behind the shoulder; then the wing is vigorously thrown forward, while releasing the thumb before the two fingers.

The initial lift Q is now directed upward. At sufficient initial speed of translation and rotation, the resultant of the mean aerodynamic resistance R and of the weight is an upwardly directed force, hence an upwardly directed concavity for the trajectory. At point I of the trajectory, where the tangent is vertical, the conditions are similar to the initial conditions of launching by the conventional method, with a vertical speed of projection. The trajectory forms thus a complete loop, as represented in figure 29. This motion is, of course, possible only when the wing is given an initial speed high enough to reach point I. In the contrary case the trajectory is inflected at a point marked I on the lower curve of figure 29, the point beyond which the concavity of the trajectory remains downward.

4. Vertical Launching

The wing is released without speed in its own vertical plane, its large side being horizontal. The trajectory of the center of gravity cannot be kept vertical indefinitely, even in still air; it curves inward immediately at the same time as the rotation starts, to be joined asymptotically to the sloping straight line of the steady motion.

Under the effect of the quickly attained speed, the least asymmetry or the least incidence of the wing becomes sufficient to start a rotation of the wing, which is accelerated under the action of the aerodynamic couple, and so much more rapidly as the prior vertical fall has been prolonged. Thus the speed of rotation impressed on the wing can be high enough to give rise, in the first half-revolution, to loops, which disappear, in the steady motion, if the latter does not permit it.

CHAPTER VIII

PADDLE WHEELS

The experiments included paddle wheels consisting of identical, angularly equidistant vanes mounted radially around an axis. The characteristics are shown in table VIII. The measurement of the angular differences made successively in the time interval by an index mark placed on a section indicates that the rotation is speeded up, starting from the launching on the platform, as in the case of the single wing.

The motion photograph of the steady motion shows an asymmetry in the half-periods (60°), the limits of which correspond to the positions normal to PQ of one of the vanes (three in the case analyzed). From H to I (fig. 30) the curvature of the envelope is greater than from I to J. This asymmetry recurs again at a complete revolution of the paddle wheel. The translation between A and P is greater than that between P and Q.

For the first half-period preceding I, the energy of couple Γ (theoretical energy of resistance to pure translation) for the blade GA (from 30° to 90° incidence) is motive energy (area a' a b c d (fig. 31)); the energy for the blade GC is resisting; blade GB is in the slipstream; hence an excess of motive energy (area a b c e). For the following half-period the motive energy for blade GA and the resisting energy for blade GB may be regarded as compensating each other; the resistance predominates on blade GC; the energy of the latter, first resisting (area a' e f g o), becomes then motive energy (area o g a a'); there still is an excess of motive energy (area g a e f). The excess of motive energy over the whole period is gaged by the shaded area; this energy of couple Γ in a complete period corresponds to the upkeep of the rotation.

The envelope of a paddle of a four-blade paddle wheel is formed by very incomplete arches by reason of a very substantial sliding motion. On applying the formula which approximately defines the limit points of the visible part of the envelope $\left(\cos \varphi = \frac{a\omega}{V}\right)$, to the 1.90 meter height level, it is found that the arch just about corresponds to a rotation of the wing of 52° only. This result checks with the photographs.

The theoretical energy of the resistance to forward motion for one period (90°, fig. 34) is motive energy for paddle GA (area o g a b c d, fig. 31); it is resisting for the paddle GD (area d c e f g o). The motive energy on paddle GB and the resisting energy on paddle GC may again be regarded as compensating. The last two paddles being in the slipstream, the air resistance predominates on the first two, hence the excess of motive energy represented by the shaded area in figure 31.

Prisms

Regular prisms, of the characteristics indicated in table IX, launched from the platform with a low speed of rotation, give rise to the same primordial phenomena as the single wings and the paddle wheels.

For the equilateral triangular prism, the photograph of the envelope of a rectilinear index mark disposed according to a height of the principal section (fig. 35), gives for a 180° rotation an incomplete arch with uneven ends; the long branch corresponds to the displacement of the characteristic point between center of gravity and apex of the triangle. The upkeep of the motion is still attributable to the inertia of the motions.

During a half-period starting from 1, the face AC alone catches the wind; for 30° the motive energy of the resistance of translation (area h' h d, fig. 31) is balanced by the resisting energy over the following thirty degrees (area d h h'). For the other half-period, the energy corresponding to the same face is resisting (area h' h c f g o); but the energy on face BC is motive energy (area o g a c h h'). There is an excess of motive energy, indicated by the shaded area.

For the quadrangular prism, the energy of the resistance over a period is resisting for the face AB and motive for the face AD. The shaded area again represents the energy of sustention (figs. 31 and 36).

Case of Circular Cylinder: Special Experiment

A circular cylinder is released with initial rotation, obtained by previous rolling on an inclined plane. The Magnus effect deflects the trajectory of the center of gravity downward, which farther on presents an inflection point, as indicated in figure 37. In this motion the cylinder counterrolls on a surface which is asymptotic in a vertical plane; the unsustained rotation tends toward zero.

CHAPTER IX

BENDING

The excessively elongated wings bend during falling; for the light paper wings, the bending occurs at $k > 5$. Torsion may even accompany bending. A slight initial curvature of the large axis induces bending which grows progressively with the angular speed.

The envelopes obtained by camera are difficult to interpret. To locate the wing at different instants during falling, it is necessary to blacken it and provide white paper index marks as indicated in figure 38.

The mean trajectory of the center of gravity is always the line of maximum slope of an inclined plane (fig. 39). In A the small sides of the wing are normal to the wind, and the concavity of the wing is turned toward the bottom of the inclined plane. In C, after a rotation of a half-revolution, the concavity is turned upward. In E, after a rotation of one revolution, the wing reassumes the same position with respect to the plane as in A. The wing curvature remains the same. The period is a complete revolution.

The arches of the envelope corresponding to two consecutive half-revolutions appear very uneven. In reality, the small forward sides of the wing, fixed by the photograph, are close together in A and C, due to the rotation about an axis upstream from A and downstream from C. Contrariwise, they are farther apart in C and E where the corresponding axes of rotation are beyond C and upstream from E. The index mark, placed along the small axis of the wing, encloses a strongly undulated curve, visible in figure 39.

At incipient bending during falling, the curvature of the wing increases under the action of the centrifugal forces due to the rotation. The curvature cannot remain constant at each instant, in steady motion. Even when assuming V and ω constant, the position of the wing with respect to the wind causes a variation in bending. From A to B, the resistance R, adding its effect to that of the central centrifugal force F_1, increases the deflection of the wing; it is the same from D to E. This effect gives a maximum curvature in A and in E. From B to D, on the other hand, R being opposed to F_1 and increasing F_2, produces a decrease in bending moment and a correlative decrease in the wing curvature, which is minimum in C.

After its passage to A, the wing straightens out again; the section is shifted backward and the trajectory of G_1, deflected suddenly upward, increases the curvature.

Comparing the wing to a portion of a circular cylinder of radius R, 2θ being the angle of the two extreme angles of the directrix, the distance of center O of the wing (of span 2b) to the axis of rotation is

$$OG = b \frac{(\theta - \sin \theta)}{\theta^2}$$

The point O passes alternatively and periodically above, then below the mean inclined plane.

The photograph in figure 40 refers to a wing provided with the index marks of figure 38; its general characteristics are: $2a = 9$ centimeters, $2b = 44.5$ centimeters, and $\Delta = 9.92$ grams per decimeter^2. The results are: AC = 43 centimeters, and CE = 16 centimeters; the deflection in A being 7.4 centimeters, and in C, 4.4 centimeters.

CHAPTER X

CURVED WINGS

The case involved is that of a wing whose "profile," instead of being straight is now circular (circular arc). The surface of the wing becomes cylindrical. The curvature of the wing is defined by the rise of the circular arc. For such wings a steady motion of descent of the kind discussed in the foregoing is not stable except when the rise is small. For instance, a 25 × 10 centimeter wing, weighing 2.04 grams per decimeter^2 has no stable steady motion if the depth of camber exceeds 1.7 centimeters.

The period comprises two half-revolutions (fig. 41) which constitutes an analogy between the envelope arches obtained in the actual case and those of the deflected wings. From A to D the convex side of the wing faces the relative wind, from D to E, the concave side. The convex side again faces the wind from E to C. The arch corresponding to the first half revolution AB is much longer than the second BC, with a flatter mean curvature.

For the afore mentioned wing (25 × 10 centimeters), with 0.7 centimeter depth of camber, the two arches GH and HK have a span of 23.8 centimeters and 19.8 centimeters, respectively. For the same wing, but flat, the span of the arches was uniformly 21.5 centimeters. For a 33 × 15 centimeter wing weighing 7.38 grams per decimeter^2 the span of the arches is 64 centimeters and 43 centimeters (fig. 42) for 1.9 centimeter height of camber; 40 centimeters for the flat wing.

Along the shortest arch, the curvature of the wing and its envelope have the same sign and also similar numerical magnitudes. The contact of the envelope and of the enveloped is of a high order, particularly in the neighborhood of E; in consequence the envelope appears as a very thick black line on the negatives.

The peculiarities of this form of the envelope can be roughly explained according to the aerodynamic characteristics of thin, circular-arc airfoils (reference 6, p. 52).

At H, the resistance to translation is maximum; applied from H to E at short distance from the center, this resistance decelerates the rotation more than it does the translation, hence, the slightly greater curvature of the arch between H and E than downstream from E. Near E, the motion appears to approach a pure sliding motion, with a minimum disturbance of the fluid. As soon as the incidences are clearly negative (relative wind on the convex face), the resistance approaches the leading edge of the wing, and its moment with respect to the center of gravity is greater here than for the positive incidences of the same absolute value: after that a rapid acceleration of the rotation. Along GD the rotation is slowed down by a very high moment couple. The deceleration persists downstream from D as far as point N where the center of thrust passes to the leading edge (relative wind on the concave face). The slight curvature of the arc DH is due to the fact that at low positive incidence the resistance is applied to the rear half of the surface.

The several negatives obtained gave the same geometric peculiarities for the two arches of the envelope.

CHAPTER XI

STABILITY

In the steady motion of falling with a wing rotating about one of its principal axes of inertia Gx and Gy (fig. 43), the equilibrium of the forces and moments is on an average established in one period. But for such a steady motion to take place effectively, the stability is a necessary condition.

Experience indicates that a rotation impressed on a wing about the mean axis of inertia Gx cannot be maintained in a stable steady motion of descent; the wing tends to fall quickly with erratic motions. By averaging enough initial speed of rotation, several half-revolutions of the wing may be obtained, an unsteady motion of the sort which enabled the curves of figures 10, 11, and 12 to be plotted corresponding to $k < 1$; in no way is it possible to fit it in the scheme of steady motion. On the contrary, every result based on the preceding studies is proof of the stability of the steady motion at rotation about axis Gy; a new one can be produced the following way:

Assume that the wing, placed on the horizontal launching platform, is given an initial rotation about a straight line of its plane parallel to the platform rim D and forming an angle u with Gy (fig. 43). The negatives show that the center of gravity, at the beginning of the fall, still describes, on the average, a straight line normal to D and

sloped at an angle α with respect to the horizon. The axis Gy describes about G a small cone of quasi-uniform motion defining a period of nutation. This period of nutation, at least when k is great, has a value several times the period of rotation of the wing. On the negatives the envelope arches follow along a wavy line with little difference from the straight line of the inclination α which remains the mean trajectory of the center of gravity. But this nutation and these oscillations are quickly damped, and Gy ultimately resumes a horizontal direction normal to the mean trajectory with the rotation continuing about this axis until the normal motion is established.

During the disturbed period of motion, the center of gravity is always animated by an oscillatory motion analogous to that which it represents in the established normal motion; as a result, the end of the great axis which follows the same oscillation fluctuates about its mean trajectory, itself oscillatory along the mean inclined plane due to the nutation. Figure 43 represents, at the right, the contour of this trajectory, plotted according to the photographs.

In this same transitory period, the aerodynamic resultant is no longer situated in the plane of symmetry Gx of the wing; the resultant moment with respect to G, which in steady motion is directed along Gy, has now a component P along Gx. When Gx is parallel to the inclined plane, the couple P governs the amplitude of the oscillations which may be called rolling oscillations of the wing (angular oscillations about the trajectory of the center of gravity; one wing tip rises above the inclined plane while the other drops below). When Gx is normal to the inclined plane, P governs the yawing moment of the wing (oscillation about an axis located in the mean plane of the trajectory of G and normal to it). Figure 43 represents, at the left, the yawing oscillations (fig. 44). In all cases, rolling and yawing have small angular amplitudes; to each angular difference of a specific sign there corresponds, one half-period later, a difference of the same value and of opposite sign; the corresponding couples P, equal and of opposite signs, have a zero mean value.

The preceding action is superposed by a damping effect (an action roughly proportional to the speeds) which reduces yawing and rolling and finally stabilizes the motion with the axis Gy horizontal in the inclined plane.

With H_0 indicating the height of launching and u the initial setting, table X gives the number of revolutions n, starting from height level H, over which an oscillation of Gy is sustained.

Joukowsky, after studying the disturbed motion of the center of gravity, concluded that the latter approaches the rectilinear trajectory either asymptotically ($\alpha > 70^\circ 32'$) or by oscillations ($\alpha < 70^\circ 32'$). No trace of such oscillations was found on any of the negatives. The

only oscillations encountered are those discussed in chapter V. And these, resulting from the variation of the instantaneous resistance R over the period of a half-revolution, appear essentially different from those described by Joukowsky.

CHAPTER XII

ISOSCELES TRAPEZOIDS

The existence of a maximum speed recognized from a study of the normal motion of fall of rectangles of span 2b led to a summary consideration of isosceles trapezoids, obtained by a slight reduction of one of the small sides of the rectangle.

On conceding that each section of the wing, comprised between two parallels to the bases of the trapezoid, corresponds to part of a rectangle of the same chord and span 2b, a speed of rotation V near the average values V_1 and V_2 characteristic of rectangles of the same span 2b and respective chord 2A and 2a, measured at the large and small base of the trapezoid, can be predicted for the trapezoid. We put $k = \frac{b}{A}$ and $K = \frac{b}{a}$ $(K > k)$.

When the straight line GI, parallel to the bases, is the principal large axis of inertia (fig. 45), and the launching is suitable for readying the rotation, the mean trajectory of G is still the line of maximum slope of an inclined plane. This case differs from the problem already treated only by the unevenness of the successive arches. The period of motion corresponds to a complete revolution.

If, on the other hand, the large principal axis of inertia is the straight line GO, the trapezoid assumes a steady descending motion, with rotation about this straight line; but the mean trajectory of G is then, as a rule, a helix outlined on a cylinder of revolution with vertical axis D. This vertical axis cannot be registered with precision except in the case of small trapezoids of light paper; with these it was possible to effect a sufficient number of revolutions about this axis at the height of fall at disposal in the laboratory.

The axis OO' turns with, on the average, a constant angular speed u about D. In this motion the points O and O' projected on the horizontal plane describe, on the average, two circles centered on D and of radius R and r. It is natural to admit, to begin with, that R must be greater than r, or in other words, that the small base is always turned toward the axis D of the cylinder. The existence and the conditions of maximum

speed described in chapter IV make the generality of the fact doubtful, and desirable to predict the conditions for which the orientation of the trapezoid must be reversed.

Let k' denote the aspect ratio corresponding to the maximum speed of translation of a family of rectangular wings of common span $2b$. If $k' > K > k$ for the trapezoidal wing in question, it may be asserted that the speed of translation is increasing for the corresponding rectangles whose chord decreases from $2A$ to $2a$: in these conditions it is natural to imagine that the large chord is inside, the small one, outside, that is, that $R < r$.

These precisions have been confirmed by experience, and it was possible to obtain, in the desired conditions, very stable helicoidal falls with the large chord of the trapezoid located on the inside.

Helicoidal falls with $R < r$ have been obtained in all cases, on trapezoids of very dissimilar ratios of k and K but always smaller than k'. However, if k' is a little greater than unity, stable rotations are difficult to obtain, which explains the fact that k is then necessarily small or even less than unity.

Conversely, for $k' < k < K$, R should be greater than r, the habitual helicoidal fall, with the small chord of the trapezoid on the inside. This also has been confirmed by experiment.

Lastly, for $k < k' < K$, the two previous modes of fall were obtained, as well as the falls in the inclined plane ($R = r = \infty$) which were, moreover, very stable. The last result, quite unexpected for trapezoids with uneven chords, is easily explained in the case where the chords differ only slightly. Table XI gives some numerical results.

The axis of rotation of the wing describes a regular helicoid with director cone, the directrixes of which are the helix described by G and the vertical axis of the same helix; the acute angle which with this axis forms the axis of rotation, is open toward the top. Due to the fact that this angle is different from 90°, the axis of rotation is not orthogonal to the direction of the speed of G, hence an oblique angle of attack of the wing with the relative wind, which must have its reflection in the laws of motion.

CHAPTER XIII

ROTATION OF GRAPHITE FLAKES IN A VERTICAL ASCENDING WIND

Screened graphite flakes are introduced in a vertical pipe into which flows the air from a wind tunnel. The wind discharges into free air through a vertical cylindrical nozzle of 1.32-centimeter diameter. In this air current the flakes rise while turning, up to the jet exit, then fall again. The rotation, which was recorded by camera, is, moreover, plainly visible to the eye.

Figure 46 shows a vertical plane passing through the axis of the nozzle, the observation being limited to the flakes whose trajectory remains approximately in this plane, the only ones whose envelopes are distinct on the negative. The flakes are seen to turn about the line of vision, in one or the other direction, at the same time as the visible effect of a force appears to prevent the flakes from rising vertically to the pipe outlet.

The determination of the motion elements of the particle with respect to the air is rendered very difficult in the experimental conditions by the calibration of the air blast; the effect of rotation of the flake (deviation of the trajectory with respect to the vertical) is supplemented by that of the divergence of the streamlines. These two effects are cumulative on both sides of the axis, where the rotations are of opposite signs; the rotation at the left of the axis (fig. 46) is clockwise, at the right, counterclockwise.

The vertical speed V in the air flow decreases when the point moves away from the orifice and at the same time from the axis of the jet. The position of the flake, at which this speed V is equal to the vertical projection v of the speed of the flake with respect to the air, corresponds to the apex of the trajectory. Above this position, the airspeed becomes less and less perceptible, the flake assumes a descending motion which tends toward the steady motion of fall (still air).

The photographs allow for these facts and show the regular succession of envelope arches which contract toward the apex of the trajectory.

Confetti, 3.9 millimeters in diameter, produces the same results.

To the case of the flakes revolving about an axis normal to the line of vision, there correspond the records of the trajectories devoid of luminous periodicity.

Similar results are obtained by spreading graphite flakes near the air holes of a lighted Bunsen burner; the flakes are carried off by the flame in red heat (fig. 47). Every bright line visible on the photograph represents an arch of the trajectory.

Photographing the trajectories is difficult because the red hot flakes are blended with the flame which, in spite of all the precautions taken, remains tinged. The curvature of the envelopes cannot be discerned here, nor the sign of the rotations be identified.

Reference is also made to the sparks which fly up in the hot air from a chimney; their trajectories appear like luminous dashes, explainable by the rotation.

Lastly, the same phenomena were encountered with mica or aluminum scale introduced in a vertical air current; but it was not possible to obtain negatives on which the directions of rotation could be identified.

CHAPTER XIV

FALL IN WATER

The sole purpose, in this concluding chapter, is to demonstrate, by experiment, the similarity existing between the rotation of wings in free fall in the air and the analogous phenomenon produced in water, to end with the general conclusion that the fall of a rectangular wing in any fluid of low viscosity gives rise to steady motions which are completely defined for every fluid by the characteristics Δ, a, k of the wing. (Throughout this chapter, Δ designates the apparent wing loading, that is to say, a deduction made from Archimedes' principle.)

These experiments were made in a tank of rectangular section, 200 × 65 × 80 centimeters in size, with the 80 centimeter dimension being the depth of the water. The temperature of the water was kept constant at about 13° for the comparison of the measurements. The photographs were taken with the camera set before one of the long sides of the tank fitted in the center with a glass window 80 × 90 centimeters (14 millimeters thick). Launching was effected from a completely immersed platform whose edge is parallel to the small side of the tank. The mean plane of the trajectories coincides with the large plane of symmetry of the tank, in which a submerged white reference mark fixes the scale of the lengths, and a plumb line the vertical. Above the tank and near this plane of symmetry, a 1-kilowatt lamp provides adequate lighting for the wings, which are painted white. The chronograph is placed above the tank.

The span 2b of the tested wings is small enough to free the rotation from any wall interference effect.

To obtain stable descent in rotation on the inclined plane requires a relatively high apparent wing loading. For instance, a 30 × 8 centimeter iron plate of an apparent weight equal to 523 grams (218 grams per decimeter^2) does not turn; two identical plates, stacked, turn but are at the limit of stable motion. The motion becomes completely stable with three plates stacked, (654 grams per decimeter^2), but the putting in steady motion also requires more than 80-centimeter depth of water.

This necessity of a value Δ higher than utilized in the air experiments without difficulty arises from the specific weight of the fluid to which the effects of the resistance are proportional.

In these conditions the thickness $2c$ of the wings, which may become true prisms, is, as a rule, no longer negligible relative to the chord; in point of fact, no sufficiently high value of Δ is obtainable except by an increase in thickness. The thickness is equal to 0.67 centimeter for the 5-centimeter-wide iron plates listed in table XII; it reaches 1.05 centimeters for the lead plates 3.5 centimeters in width. In these two cases the value for the quotient $\frac{c}{a}$ is, 0.13 and 0.3 respectively.

The lever arm should be fairly short at start of launching to insure a low initial speed of rotation; a few millimeters are sufficient. If l is too long, the resistance to launching, which increases with l, stops the plate before it has turned 90°, and the plate then slips away at high speed. This soon results in a curvature of the trajectory, then a rotation which is continued in to the stable motion if Δ is sufficient, whence the mode of launching (forward sliding motion) utilized for the wing formed by two 30 × 8 centimeter iron plates, cited in the foregoing.

Table XII gives the steady motion characteristics for several iron and lead plates.

The curves representative of α, N, and V (figs. 48, 49, 50) plotted against k have the same form as the corresponding curves for the fall in air.

The unstable motion ($k < 1$), as in the case of air, lies in the extension of the characteristic corresponding to the stable motion; but in consequence of the very substantial sliding, the exact measurements necessitate a greater depth of water than 80 centimeters.

The search for complete formulas defining the constants of the steady motion will require long series of experimentation. It is likely that the thickness will enter the formulas as a new parameter.

According to table XII, the expressions

$$E = k^{3/4}\tan\alpha \qquad F = k^{-1/5}N \qquad H = 10^{-3}\frac{V^2}{\sin\alpha}$$

are sensibly constant for the tested plates at constant chord and thickness and a specified apparent weight per decimeter^2. These expressions are of the same form as for air, except that in F, the exponent of k takes the value $-\frac{1}{5}$ in place of $-\frac{1}{3}$.

In a regular state of motion (fig. 52), the path of the center of gravity presents oscillations of high amplitude. This amplitude itself is important for wings of small dimensions. The trajectory is to a great extent identical with the envelope of the plate from which it does not break away cleanly except in the region of minimum elongation on either side of OA ($i = 90^\circ$).

The point G_1 of minimum elongation is still shifted considerably downstream with respect to OA. The asymmetry of the arches with respect to OA, which in air is appreciable only when the wings are of great dimensions, appears here for wings of small dimensions (15 × 5 centimeter wing in the table, for instance). The curvature in E (upstream from OA) is distinctly greater than that in F (downstream). The point of contact of the tangent common to the envelope arches has shifted downstream with respect to the center of the arch.

If the motion of the center of gravity was rectilinear and uniform and the rotation constant, the looped rolls of the vertexes of the wing are formed theoretically for $\frac{V}{aN} < 6.28$.

The envelope arches, for the 15 × 5 centimeters $\left(\frac{V}{aN} = 9.6\right)$ and the 30 × 5 centimeter wing $\left(\frac{V}{aN} = 6.5\right)$ in table XII, present points of inflection. For the second wing, the softly rounded region around the point of inflection is evidence of the presence of a loop, of very small area it is true, while the ratio $\frac{V}{aN}$ is higher than 6.28.

This premature formation of loops is due to the high amplitude of oscillation of the trajectory of G and to important variations of V and N during one period, and which are the result of this severe oscillation.

The speed of translation of G is minimum for a position of the section of the wing near the stationary tangent; it is seen on the successive images of the section, photographed with the electric arc; these images are severely contracted in this region, cutting off arcs of minimum length on the trajectory of G.

Quantity $\frac{V}{aN}$ varies considerably throughout the period. Very much higher than 6.28 along the arcs of light curvature, its value approaches this limit on the arc of great curvature. In the case of the 30 × 5 centimeter wing $\frac{V}{aN}$ becomes even less than 6.28 in the point of inflection. The looping depends on the $\frac{V}{aN}$ value at this point.

It was stated that the tangent OT to the point of inflection of the envelope is not perpendicular to the mean inclined plane; it is shifted downstream at an angle u with respect to the normal. For the fall in air this displacement does not appear because the envelopes for the wings employed in the tests present unreal points of inflection situated in the geometric extension of the part of the arch that is materially swept by the wing and recorded by the photograph; nevertheless, the asymmetry of the arches of the large wings raises suspicions about this particular geometric peculiarity. For the 15 × 5 centimeter and 30 × 5 centimeter wings, the angle u is equal to 5° and 6°, respectively.

Vertical Launching

As in free air, a steady motion of fall in vertical sliding is impossible. After a certain height of fall, starting from vertical launching, the path of the center of gravity curves inward, slowly at first, then very rapidly, which corresponds with the incipient rotation of the wing with the water which it encircles. The angular acceleration can assume a considerable value, resulting in a second, considerably shortened arch, with a $\frac{V}{aN}$ substantially below 6.28 and a slowing up of the fall, which disappears in the following, much longer arch.

If its inertia is inadequate, the wing is unable to perform the second quarter of the revolution, for which the resisting couple is maximum. The rotation becomes zero in an azimuth where it ushers in a new and long slide, which may end in a rotation.

Quadrangular Prisms

The necessity for giving wings sufficient thickness and inertia in order to obtain regular rotatory falls prompted the tests of square prisms.

Of the most diverse sizes and materials (brick, iron, lead, for example), these prisms give rise to perfectly regular steady motions, in water.

Sustained rotation, almost impossible on thin rectangular wings over the period of a half revolution, is easily secured here over the period of a quarter revolution. The aerodynamic couple being motive energy four times per revolution and the inertia considerable, the azimuths, where the couple is resisting, are easily passed.

With identical prisms but made of material lighter than water, steady ascending motions can be obtained, the prism having a counterrolling motion on an inclined plane located above the envelope.

Oscillating Fall

If Δ is sufficiently small and the dimensions of the plate are appropriate, the rotation may become impossible. It is then replaced by a steady motion of oscillation, the laws of which pose a new problem. The results furnished by several photographs are shown by way of example.

The envelope, viewed in projection on the plane of vision (fig. 53), is formed by a succession of equal, upwardly concave arcs, each of which corresponds to a single oscillation. In these oscillations the motion about the center of gravity is a pitching motion about the long axis of the wing, which maintains a direction that is largely fixed and horizontal; the pitching amplitude may become some 10° higher, starting from the horizontal plane.

The center of gravity, which moves in a vertical plane perpendicular to the fixed direction of the long axis, is animated by a synchronous oscillation (fig. 54). The pitching angle is regarded as positive when the advancing half wing is situated above the horizontal plane passing through the long axis. On passing the mean vertical of the fall the pitching angle of the wing, sliding toward the right, for example, is negative and increasing. Simultaneously, the angle of attack increases, which quickly raises the hydrodynamic resistance and results in the arrest of the rightward displacement of the center of gravity (horizontal speed nullified); the pitching angle is then positive and reasonably constant. The fall can but begin again; now it is toward the left, with a sliding motion which starts in a plane which is largely the plane of the wing at the preceding arresting moment (plane tangent to the end of the envelope arch). The angle of pitch is now to be considered as negative since it is the other half wing that is considered as leading the motion. The sliding is rapid at first, then, as the pitching angle increases, the horizontal speed of the center of gravity decreases, and cancels out in the same conditions as before (most leftward position of center of gravity).

The photographs of figures 53 and 54 refer to aluminum wings of 6.5 × 2.5 centimeter and 5 × 3.7 centimeter dimensions (Δ = 6.19 grams per decimeter^2), the periods of oscillations being 0.9 and 1.23 seconds.

In free air, large and light wings, abandoned in the horizontal position, give rise to a similar steady motion of fall.

An oscillating fall in which the pitching axis, instead of maintaining a fixed position as in the foregoing, turns about the mean vertical of the motion, probably by warping, is easily obtainable in water with very long plates. For a 12.7 × 1 centimeter aluminum plate, weighing 0.8 gram, this rotation is effected at the rate of one revolution for about eight complete oscillations.

Translated by J. Vanier
National Advisory Committee
for Aeronautics

REFERENCES

1. Maxwell: Scientific Papers, vol. I, pp. 115-118.

2. Mouillard: L'Empire de l'Air, p. 210. Théorie de l'Aéroplane.

3. Moedebec, H.: Taschenbuch zum praktischen Gebrauch für Flugtechniker und Luftschiffer, pp. 177-181.

4. Joukowsky: Bulletin de l'Institut aérodynamique de Koutchino, fascicule 1, 1912.

5. Bouasse: Resistance des Fluides, p. 147.

6. Eiffel: La Résistance de l'air et l'aviation, corps ronds, p. 75.

TABLE I

Δ g/dm^2	$k = \frac{b}{a}$	2a cm	2b cm	α deg	α min	N revolutions per sec	V cm/s	$\frac{V}{aN}$	E	F	H
0,14	2,66	1,5	4	42	35	9.5	80	11,2	2,14	9.79	11.7
----	3.33	-----	5	38	30	10.2	76	9.9	2.17	9.37	11.4
----	4.00	-----	6	34	50	10.8	73	9.0	2.16	9.30	11.4
1.3	6.00	2	12	32	5	11.9	106	8.9	2.85	11.1	25.2
----	3.00	3	9	42	45	7.1	114	10.7	2.75	11.4	25.2
----	3.33	-----	10	40	10	7.4	111	10.0	2.75	11.4	25.2
----	4.00	-----	12	36	40	7.9	107	9.0	2.81	11.1	25.3
----	5.00	-----	15	33	10	8.4	103	8.2	2.86	11.1	25.6
----	2.50	4	10	45	35	5.3	115	10.8	2.88	11.0	26.1
----	3.00	-----	12	41	30	5.6	109	9.7	2.86	11.0	25.3
----	2.30	5.2	12	44	25	4.4	110	9.6	2.75	11.4	26.0
----	2.00	6	12	46	10	3.8	109	9.6	2.76	11.5	25.8
----	2.33	-----	14	43	10	4.0	106	8.8	2.81	11.5	25.8
----	2.66	-----	16	39	50	4.2	102	8.1	2.75	11.5	25.4
----	3.00	-----	18	37	35	4.3	100	7.8	2.78	11.5	25.8
----	4.00	-----	24	32	10	4.7	93	6.6	2.76	11.5	25.6
----	1.50	8	12	50	5	2.7	107	9.9	2.75	11.1	25.1
2.04	3.00	3.6	10.8	44	20	7.4	159	11.9	3.70	13.5	47.3
----	4.00	-----	14.4	38	50	8.3	153	10.2	3.73	13.7	48.1
----	5.00	-----	18	33	30	8.6	142	9.4	3.03	13.2	47.1
----	3.00	5	15	41	50	5.7	152	10.7	3.09	13.4	47.8
----	2.00	6	12	49	10	4.5	156	11.6	3.13	13.5	48.8
----	2.33	-----	14	45	30	4.6	150	10.9	3.06	13.3	47.9
----	2.66	-----	16	42	45	4.7	147	10.4	3.05	13.2	48.4
----	3.00	-----	18	40	30	4.9	144	9.8	3.07	13.2	48.0
----	3.00	8	24	39	5	4.1	138	8.4	3.13	13.5	48.3
----	0.80	10	8	63	50	2.2	162	14.7	3.12	13.3	48.5
----	0.90	-----	9	61	30	2.3	160	13.9	3.07	13.4	48.3
----	1.00	-----	10	59	50	2.4	158	13.2	3.08	13.5	48.0
----	1.60	-----	16	49	50	2.8	148	10.6	3.05	13.5	47.6
----	2.00	-----	20	45	20	3.1	142	9.2	3.07	13.4	47.1
----	2.50	-----	25	41	00	3.2	138	8.6	3.09	13.3	48.1
----	3.00	-----	30	37	30	3.4	133	7.8	3.05	13.3	48.1
2.57	3.00	8.0	24.0	40	15	4.3	147	8.6	3.27	14.2	50.5
5.14	3.00	5.65	16.96	46	50	7.5	249	11.8	3.77	19.3	114.3
6.32	3.00	8.0	24.0	45	5	6.3	270	10.7	3.86	20.8	141.1
7.38	4.10	5.8	23.8	42	10	9.3	307	11.4	4.04	21.6	178.4
----	3.00	8.0	24.0	46	10	6.9	312	11.3	4.02	22.8	182.3
----	2.20	15.0	33.0	48	20	3.8	306	10.7	4.04	22.4	184.2
----	2.35	17.0	40.0	46	10	3.4	298	10.3	4.02	21.4	182.3
7.94	1.76	19.0	33.5	52	5	3.0	328	11.5	4.08	22.6	197.6
8.89	3.00	8.0	24.0	47	15	7.7	350	11.4	4.17	25.4	213.6
9.18	1.50	4.0	6.0	65	25	10.5	398	19.0	4.20	25.7	205.7
----	2.00	3.0	6.0	61	55	14.3	401	18.7	4.16	26.0	207.8
----	1.66	6.0	10.0	61	25	8.1	384	15.8	4.20	26.5	208.2
11.59	4.00	8.5	34.0	41	45	9.5	376	9.3	4.28	30.4	273.9
13.1	3.00	3.57	10.72	54	30	19	468	13.8	4.35	31.2	309.5

TABLE II

Δ g/dm^2	2b cm	$k = \frac{b}{a}$	α		N revolutions per sec	V cm/sec
			degrees	min		
1.3	12	2.00	46	10	3.8	109
---	--	2.30	44	25	4.4	110
---	--	3.00	41	30	5.6	109
---	--	4.00	36	40	7.9	107
---	--	6.00	32	5	11.9	106

TABLE III

Δ gr/dm^2	$2b \times 2a$ cm^2	α degrees	α min	V cm/s	V_1 cm/s	$\frac{V - V_1}{V}$	y_o cm	y_1 cm	β degrees
7.38	40 × 17	46	10	298	236	0.11	0.9	1.1	16
11.8	44.5 × 21	49	20	396	359	0.09	1.0	1.3	23
6.61	60 × 32	46	00	258	226	0.12	1.9	2.9	29

TABLE IV

2b × 2a cm^2	$k = \frac{b}{a}$	Δ g/dm^2	i		Ω		N rev/sec	N_2 rev/sec	$N_2 - N$ rev/sec	$\frac{N_2 - N}{N}$
			deg	min	deg	min				
33 × 15	2.2	7.38	33	10	27	45	3.8		0.4	0.11
			62	55	30	15		4.2		
			90	30	26	30				
			116	50	26	5				
40 × 17	2.35	-----	52	5	22	0	3.4		0.5	0.15
			77	25	27	45		3.9		
			103	30	24	30				
			127	30	23	25				
44.5 × 21	2.12	11.8	36	20	28	5	4.0		0.2	0.05
(Fig. 19)			65	35	30	20		4.2		
			95	15	29	0				
			123	10	26	50				
60 × 32	1.88	6.61	42	20	12	15	1.9		0.2	0.11
			55	10	13	25				
			69	5	14	30				
			84	0	15	20		2.1		
			92	20	15	20				
			99	15	15	10				
			113	0	12	25				
			125	0	11	30				

TABLE V

Δ g/dm^2	$2b \times 2a$ mm^2	$k = \frac{b}{a}$	H m	N_o rev/sec	H_1 m	H_2 m	N rev/sec
10.9	155 x 15	10.3	4.75	6.9	2.25	1.25	48.0
----	--------	----	4.00	---	2.58	2.42	25.0
----	--------	----	----	---	2.00	1.82	33.0
21.6	210 x 25	8.4	4.75	5.2	2.50	0.20	29.0
19.0	280 x 24	11.7	----	5.9	2.30	1.75	20.8
----	--------	----	----	---	2.10	0.85	26.5
----	--------	---	----	---	2.35	0.60	28.8
----	--------	---	----	---	1.65	1.15	30.0
----	--------	---	----	---	1.10	1.00	33.3

TABLE VI

COUPLE g-cm	H cm	N rev/sec	$\frac{V}{aN}$	COUPLE g-cm	H cm	N rev/sec	$\frac{V}{aN}$
120	0	3		600	0	5.8	
	8	2.5			12	3.8	
	46	2.4	10.05		33	2.9	7.54
	102	2.6	12.56		76	2.8	10.05
	163	2.7			118	2.9	
				Steady			
300	0	4.4		motion		3.0	11.50
	9	2.8					
	43	2.6	9.42				
	99	2.7	11.93				
	159	2.8					

TABLE VII

H cm	N rev/sec	V	$\frac{V}{aN}$	H cm	N rev/sec	V	$\frac{V}{aN}$
13	25.0	375	3.77	119	9.8	363	8.79
38	16.0	368	5.65	136	9.4		
60	12.2	354	6.91	Steady motion	9.5	376	9.31
74	11.3	350	7.54				

TABLE VIII

Number of Blades	2b × a cm^2	Total Weight g	H cm	N rev/sec	V cm/s	$\frac{V}{aN}$	α deg	α min
3	26 × 5.5	8.62	350(H_o)	2.3				
photo (fig. 32)			195	3.6	183	8.79	70	30
			130	4.0	214			
4	20 × 5	10.28	350(H_o)	2.0				
			190	3.8	271	14.44		
photo (fig. 33)			140	4.3			84	30
			110	4.4	300	13.82		

TABLE IX

Number of Faces	Total Weight g	Width of Face cm	Span cm	H cm	N rev/sec	V cm/s	$\frac{V}{aN}$	α deg	α min
3	15.12	14	36	350(H_o)	1.2				
				210	1.7	260			
				140		272		71	50
				90	2.0				
4	15.84	11	36	350(H_o)	1.1				
				205	1.2	173	18.21		
				138	1.6	190	15.07	71	20
				70	1.8	199	14.44		
∞	4.98	Radius 2.85	22.5	260(H_o)					
				200	2.6	226	30.77		
				150	2.4	260	38.31	80	
				128	2.3	270	41.45		

TABLE X

Δ g/dm^2	2b × 2a cm^2	u deg	u min	H_o cm	H cm	n rev/sec
2.04	14.4 × 3.6 (Photo 44)	4	00	250	120	3.0
-----	18.0 × 3.6	----	--	---	160	4.5
-----	15.0 × 5.0	7	30	---	175	2.0

TABLE XI

Δ g/dm^2	2b cm	2A cm	2a cm	$k = \frac{b}{A}$	$K = \frac{b}{a}$	k'	R − r
1.3	4.0	3.8	2.5	1.1	1.6	3.9	<0
---	---	3.4	2.3	1.2	1.7	---	<0
---	---	3.0	2.0	1.3	2.0	---	<0
---	---	2.0	1.5	2.0	2.7	---	<0
---	---	0.9	0.5	4.4	8.0	---	>0
---	---	0.8	0.5	5.0	8.0	---	>0
---	12	9.0	6.0	1.3	2.0	2.3	<0
---	---	8.0	7.0	1.5	1.7	---	<0
---	---	8.0	6.0	1.5	2.0	---	<0
---	---	6.0	4.0	2.0	3.0	---	Plan
---	---	5.7	4.5	2.1	2.7	---	Plan
---	---	4.0	2.0	3.0	6.0	---	>0
---	---	3.0	2.0	4.0	6.0	---	>0

TABLE XII

Δ g/dm^2	$k = \frac{b}{a}$	2a cm	2b cm	2c cm	α deg	α min	N rev/sec	V cm/s	$\frac{V}{aN}$	E	F	H
429	8.57	3.5	30.0	0.67	21	30	4.6	53	6.6	1.97	3.01	7.7
iron	1.50	5.0	7.5	0.67	51	20	2.4	75	12.5	1.70	2.22	7.2
	3.00	---	15.0	----	36	00	2.7	65	9.6	1.67	2.18	7.2
	6.00	---	30.0	----	24	20	3.4	55	6.5	1.73	2.24	7.3
887	1.42	3.5	5.0	1.05	57	55	5.4	130	13.8	2.08	5.05	20.0
lead	2.85	---	10.0	----	42	55	6.2	118	10.9	2.04	5.04	20.4
	5.71	---	20.0	----	29	25	7.0	100	8.2	2.09	4.96	20.4
	8.57	---	30.0	----	22	00	7.6	87	6.5	2.02	4.97	20.2

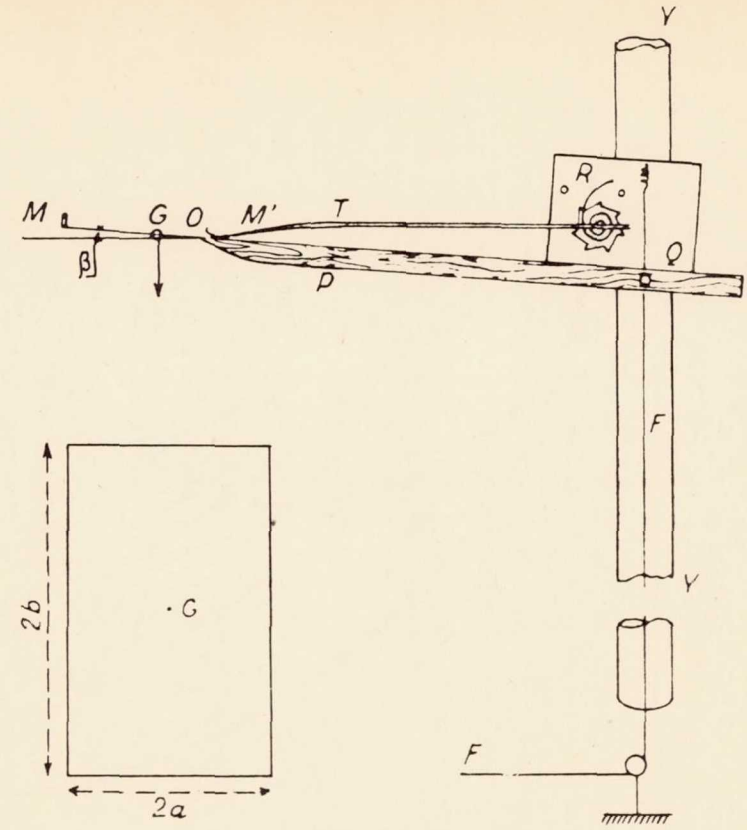

Figure 1.

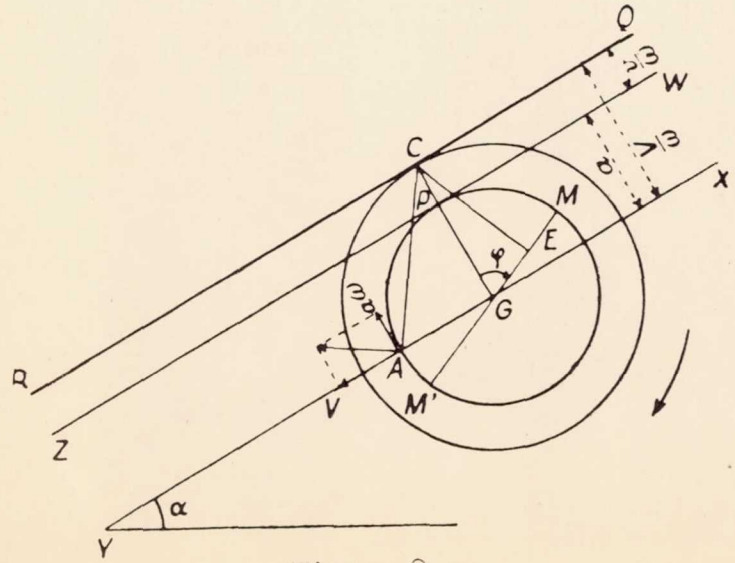

Figure 2.

Page intentionally left blank

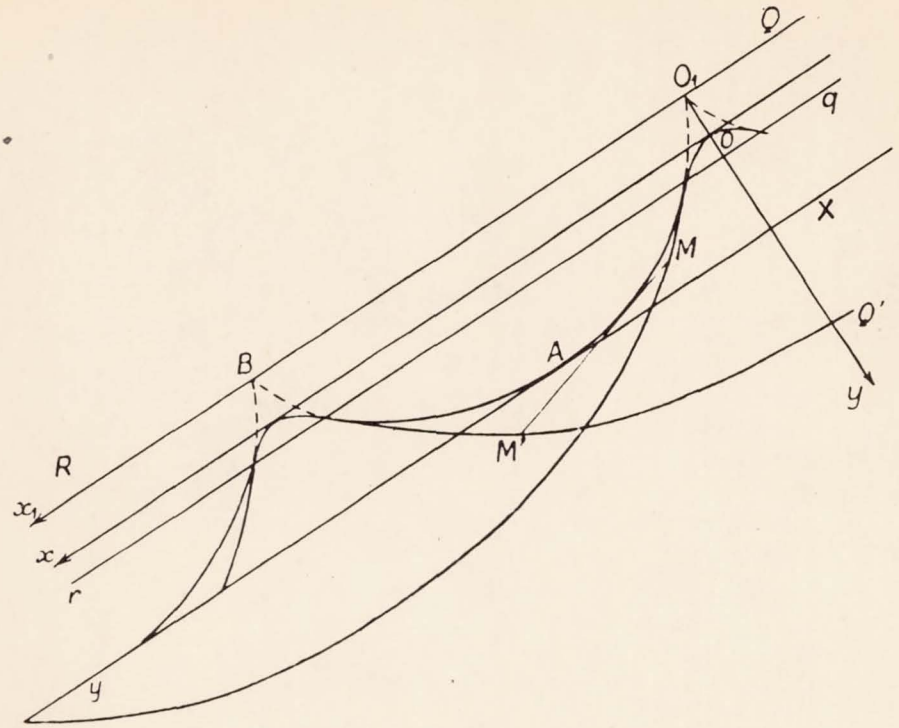

Figure 3.

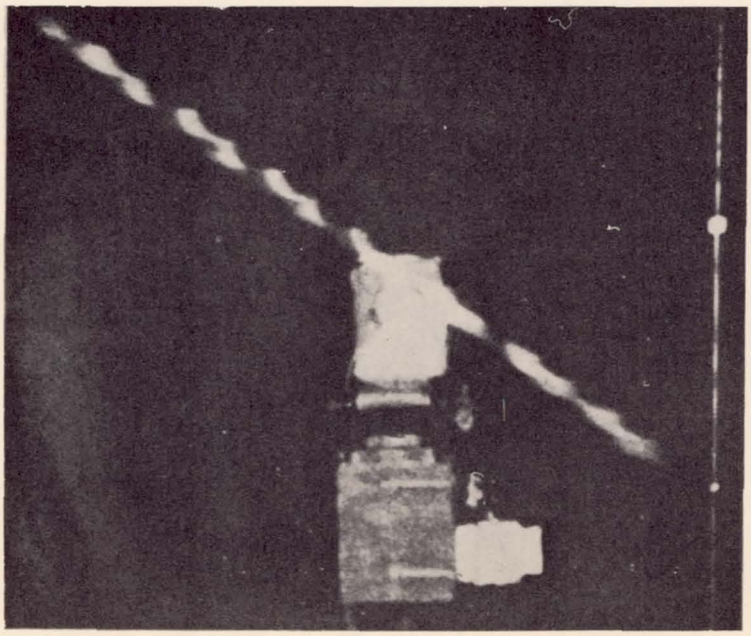

Figure 4.

Page intentionally left blank

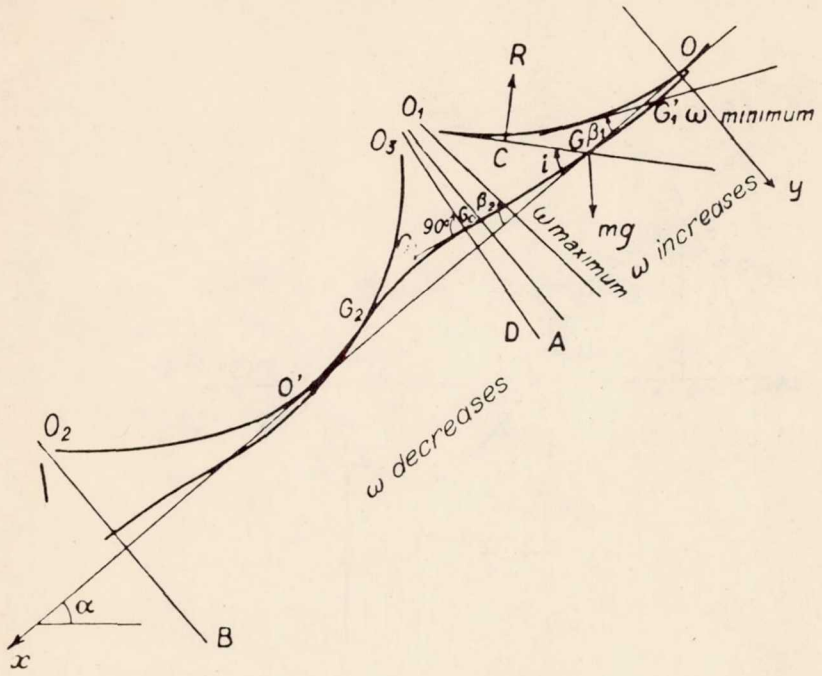

Figure 5.

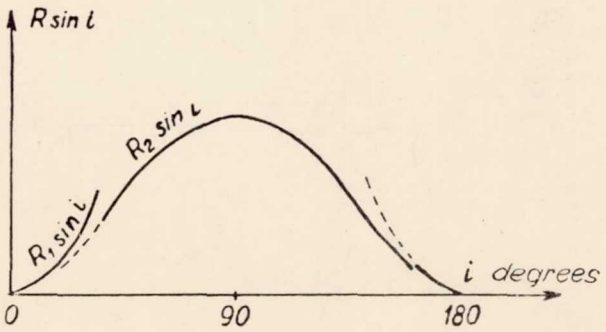

Figure 6a.

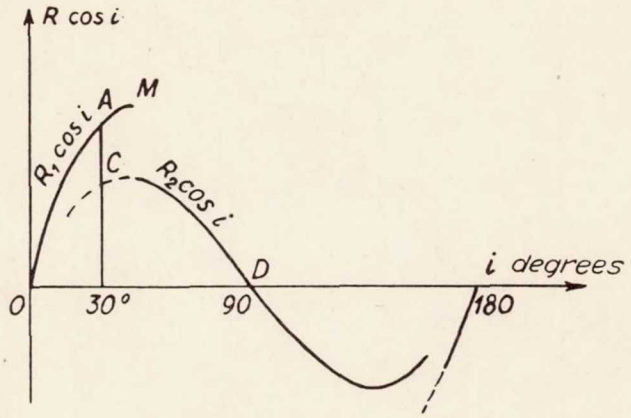

Figure 6b.

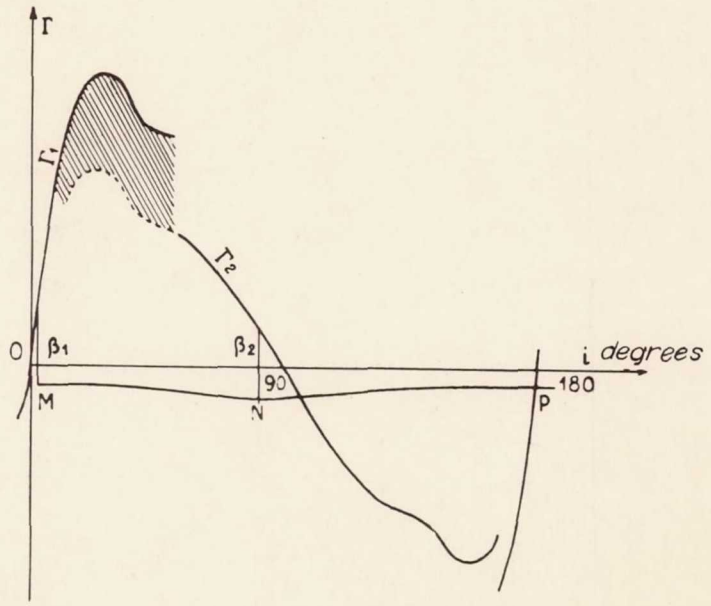

Figure 7.

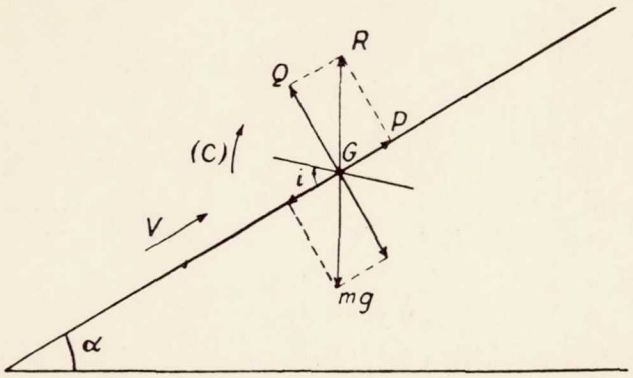

Figure 8.

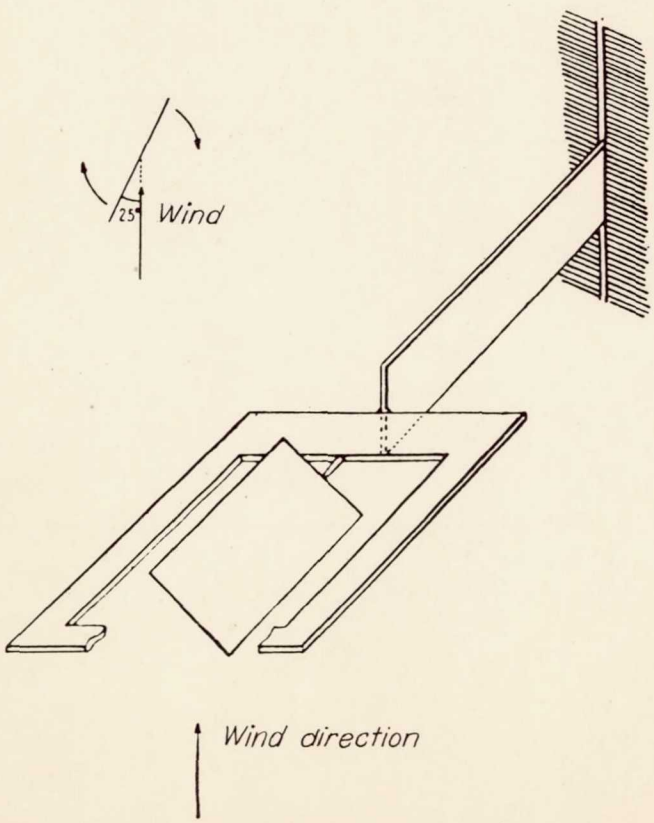

Figure 9.

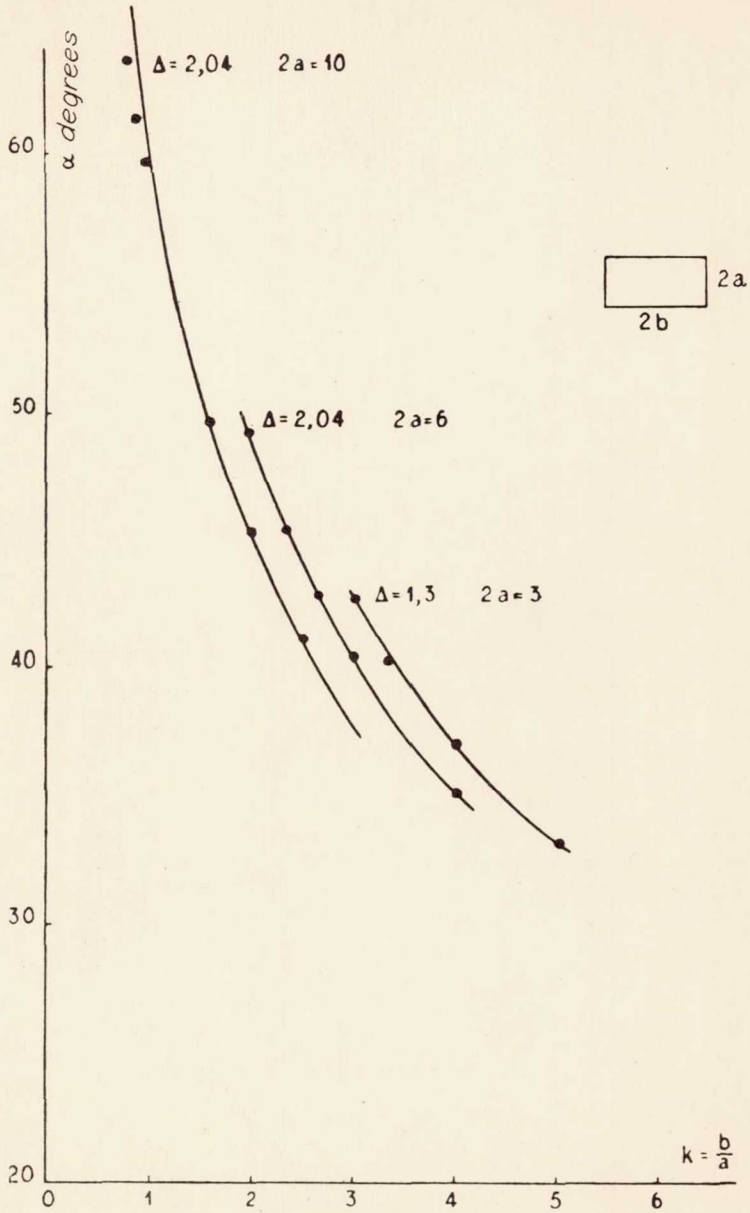
α degrees
Δ = 2,04 2a = 10
Δ = 2,04 2a = 6
Δ = 1,3 2a = 3
2a
2b
60
50
40
30
20
0
1
2
3
4
5
6
k = b/a

Figure 10.

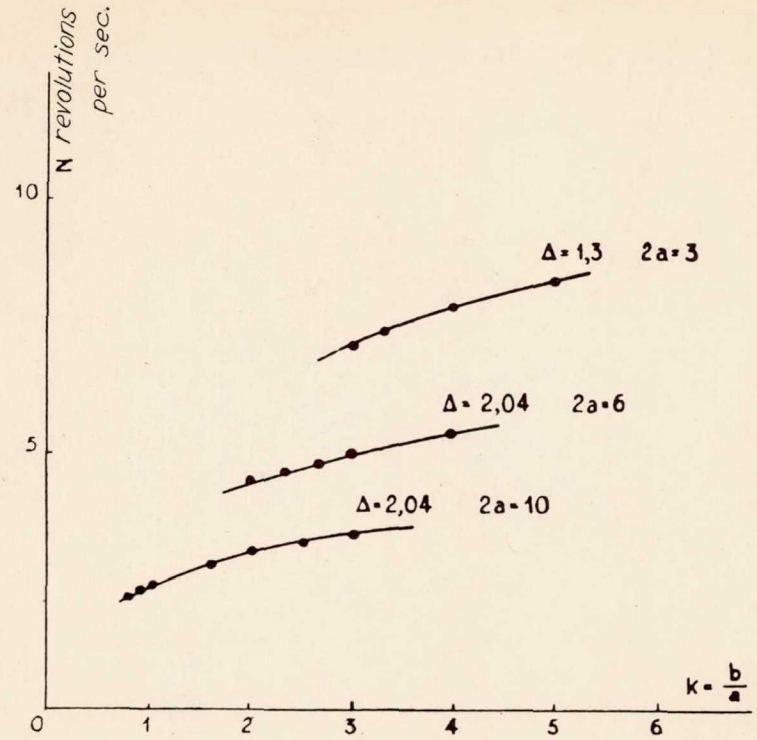

Figure 11.

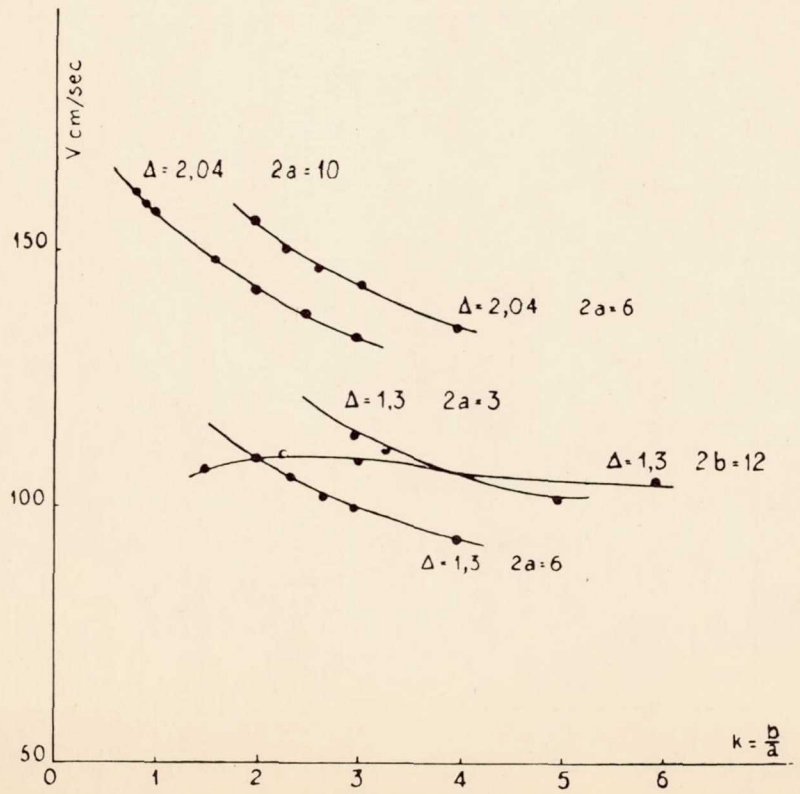

Figure 12.

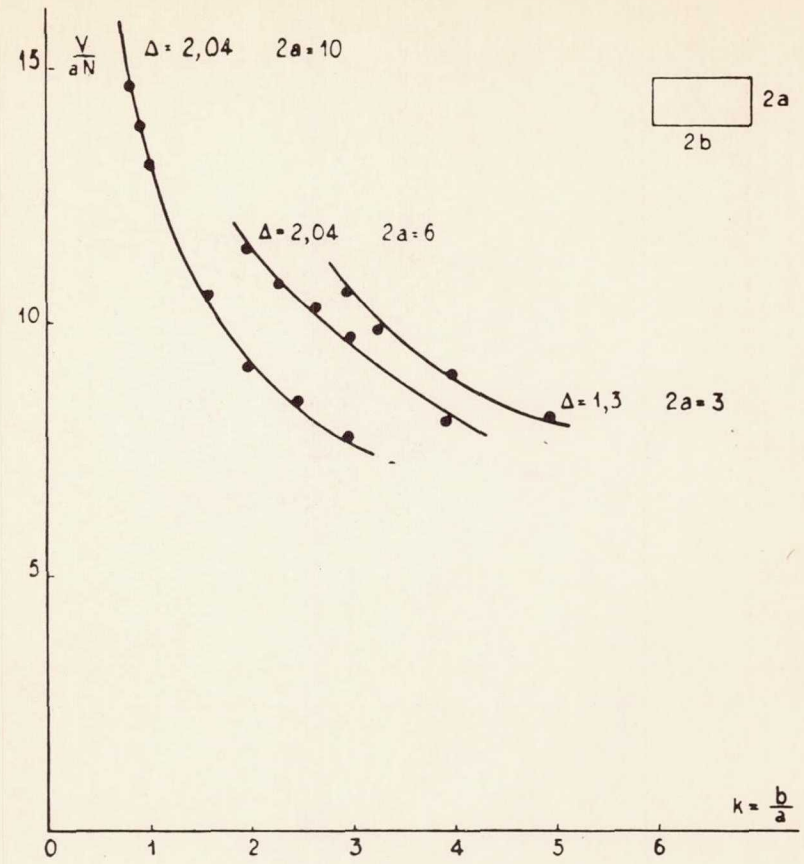

Figure 13.

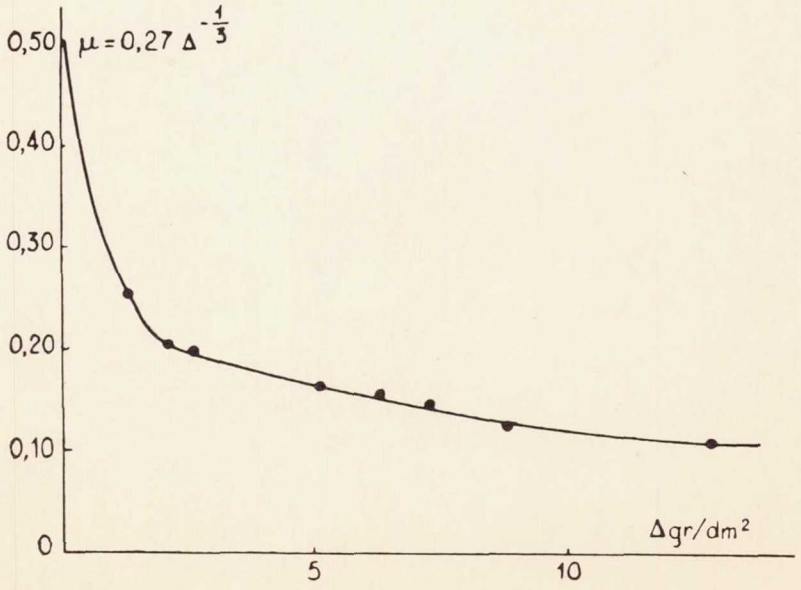

Figure 14.

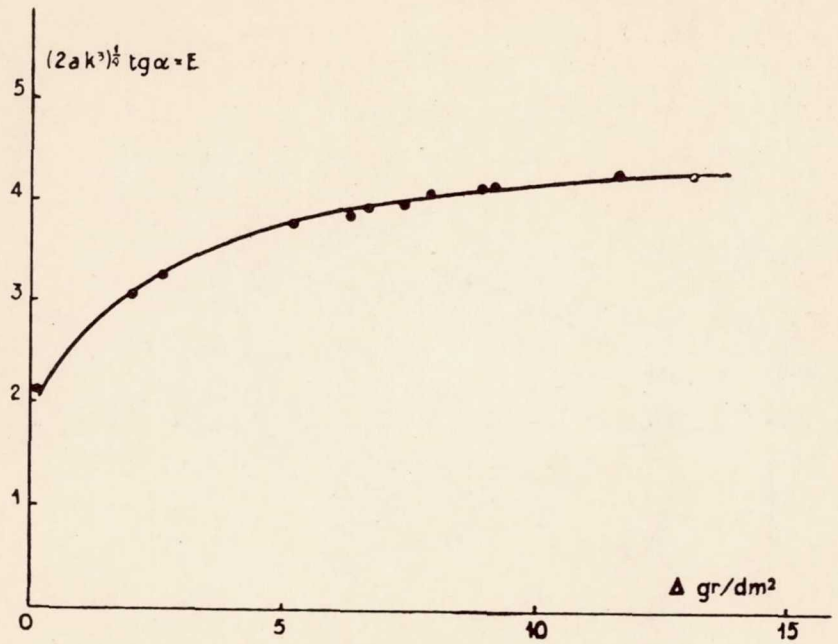

Figure 15.

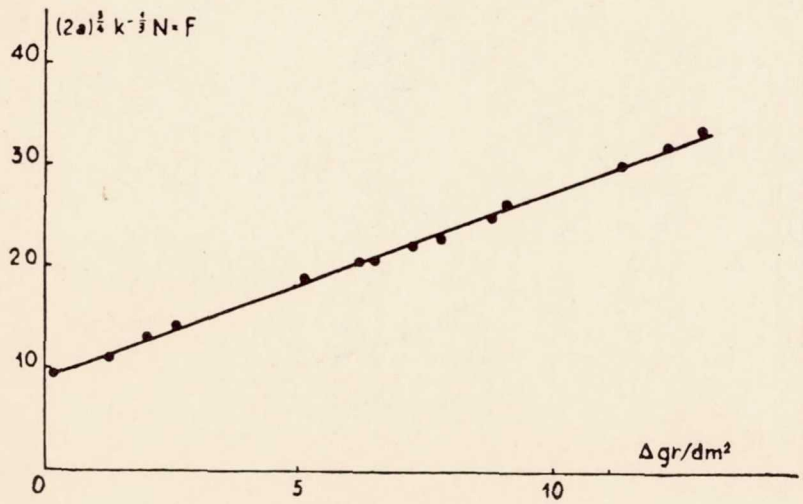

Figure 16.

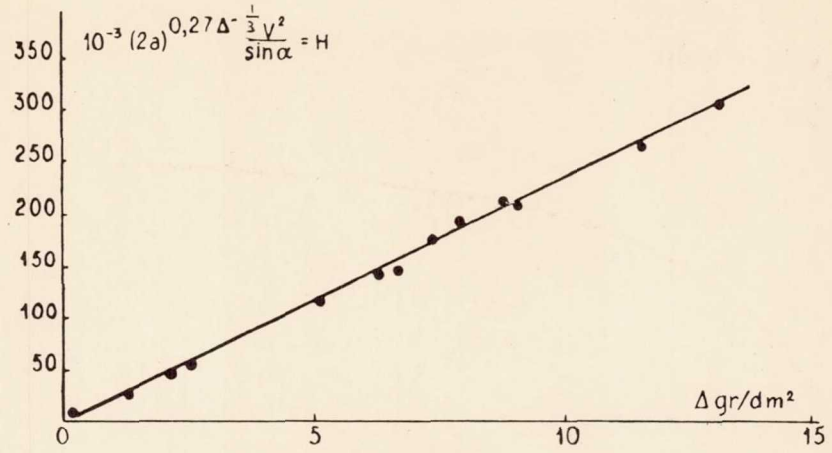

Figure 17.

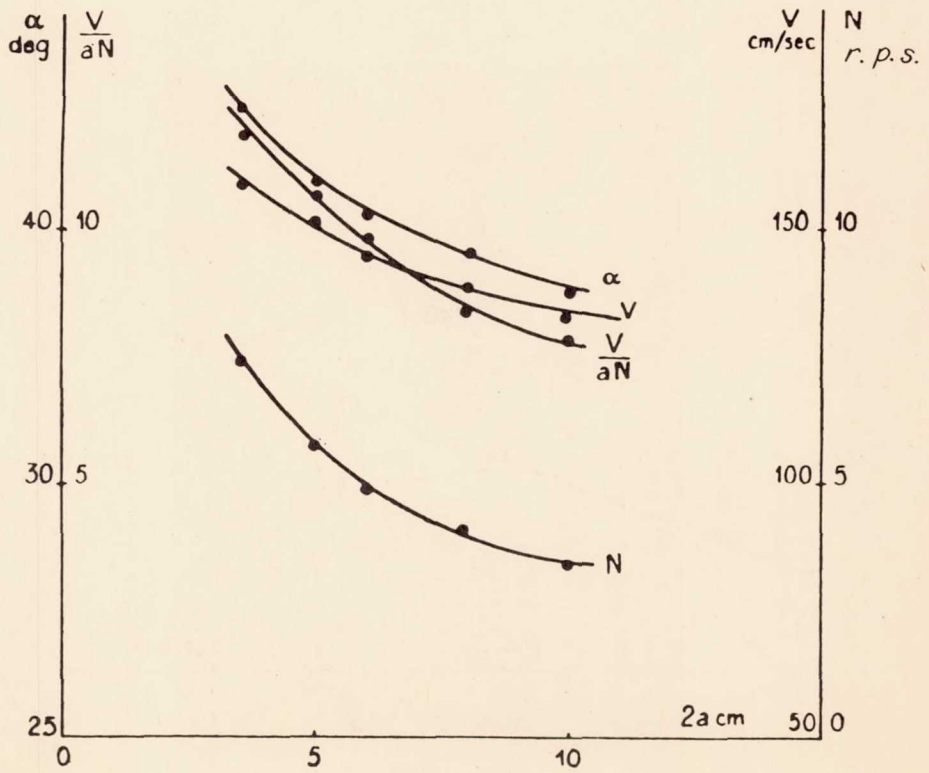

Figure 18.

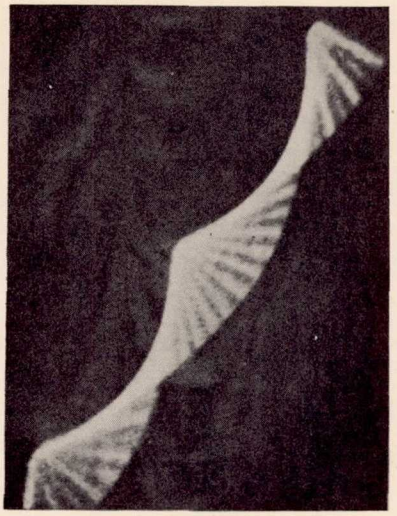

Figure 19.

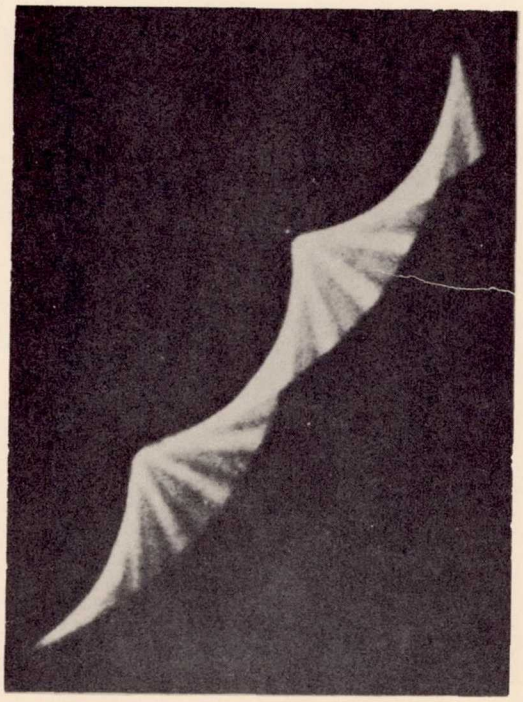

Figure 20.

Page intentionally left blank

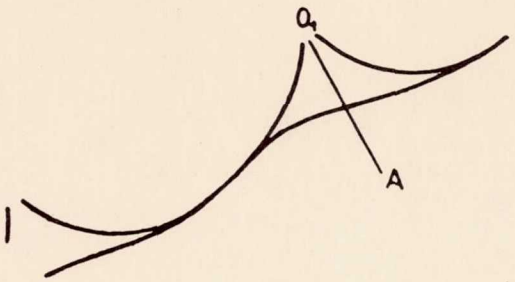

Figure 21.

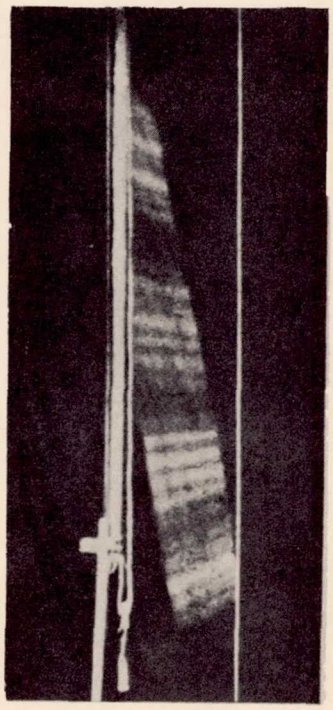

Figure 22.

Page intentionally left blank

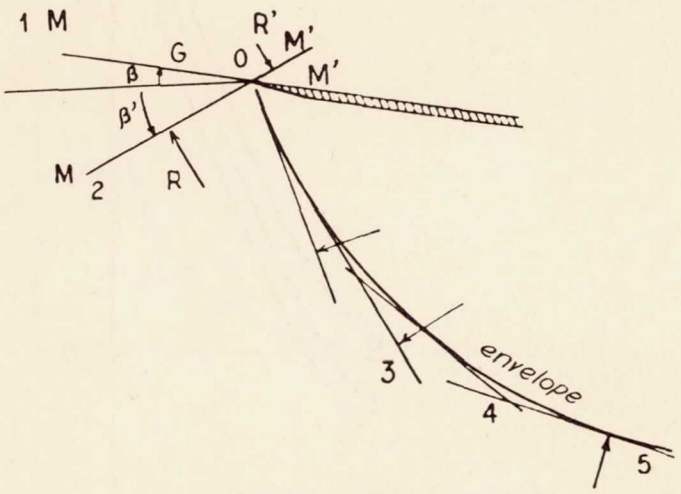

Figure 23.

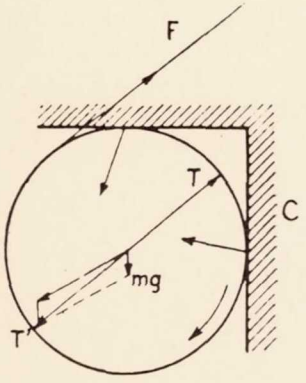

Figure 24a.

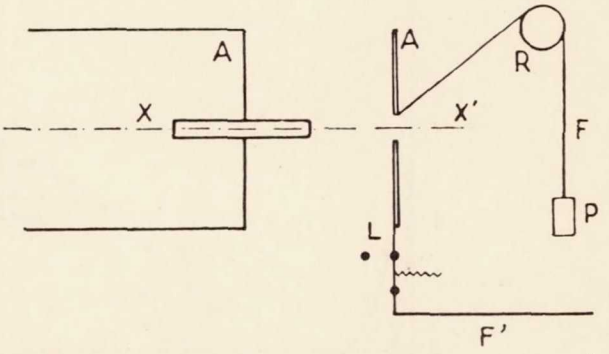

Figure 24b.

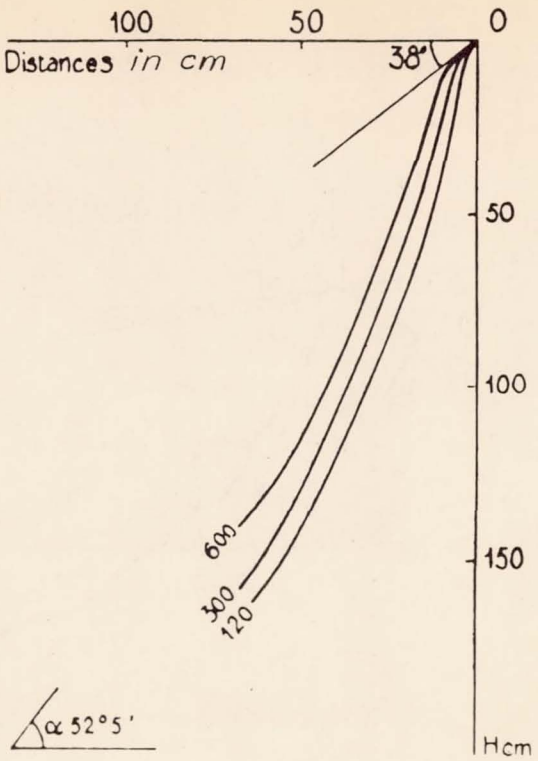

Figure 25.

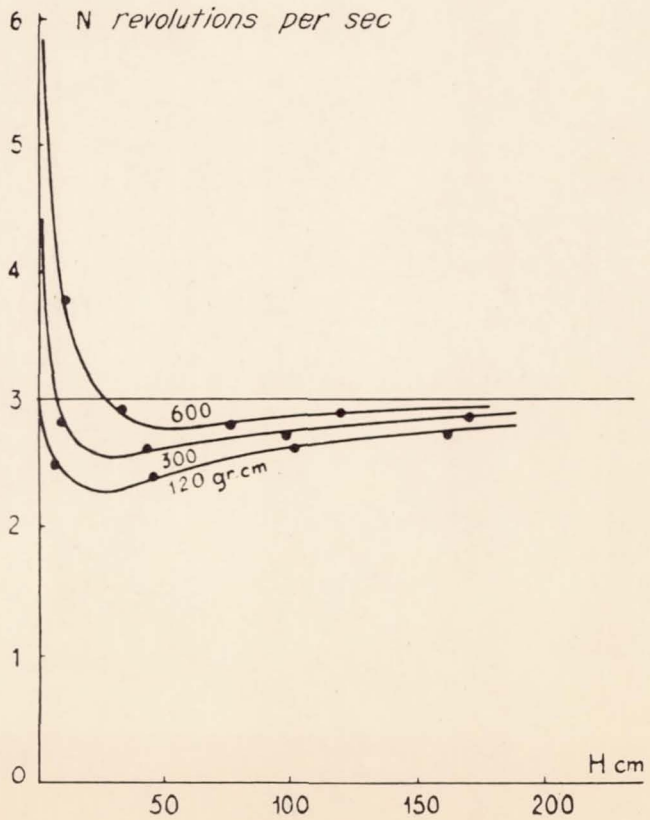

Figure 26.

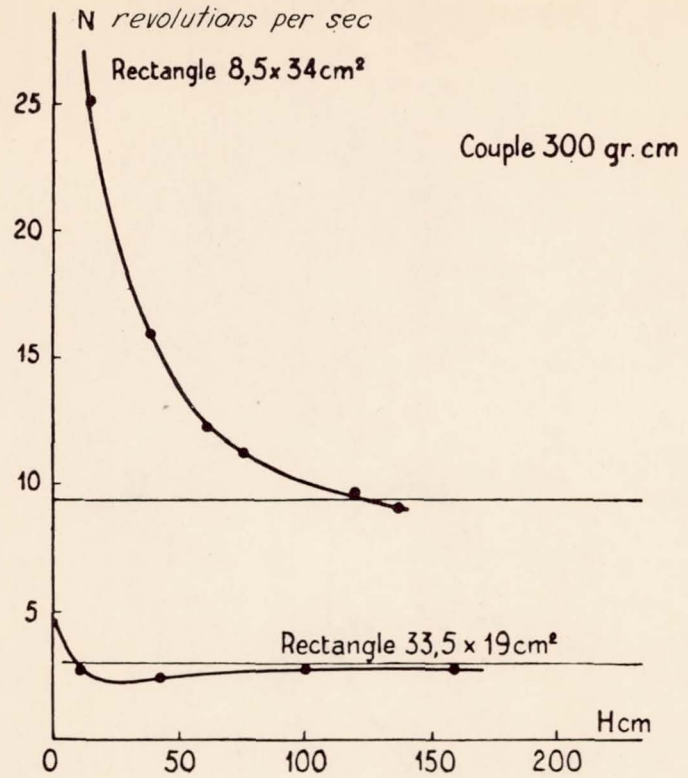

Figure 27.

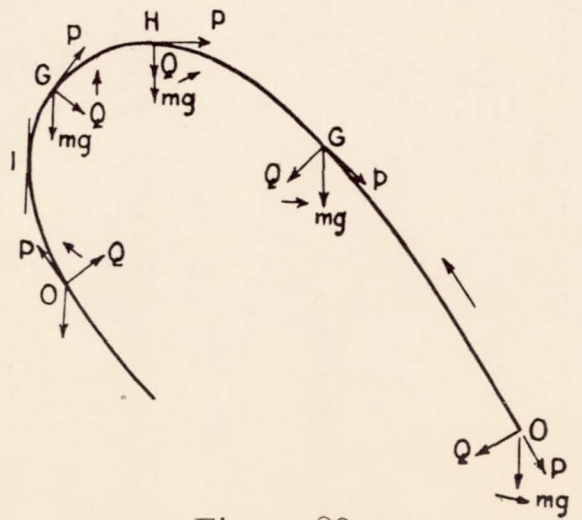

Figure 28.

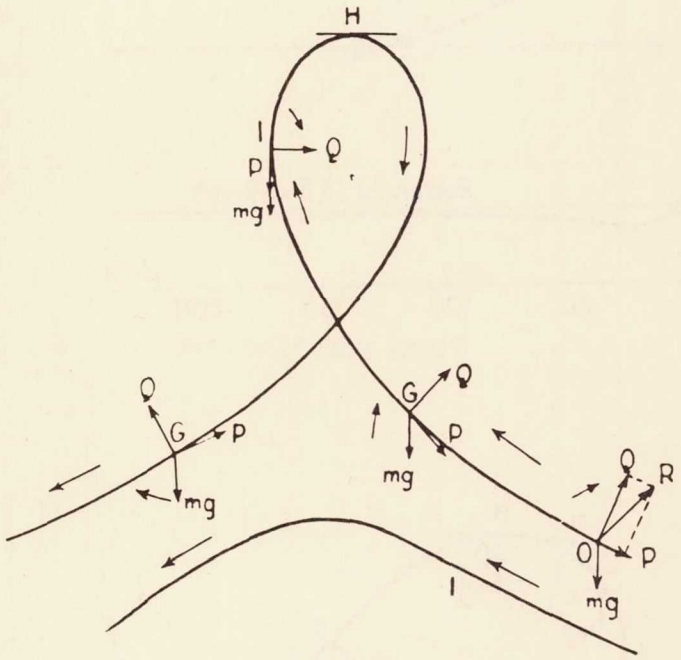

Figure 29.

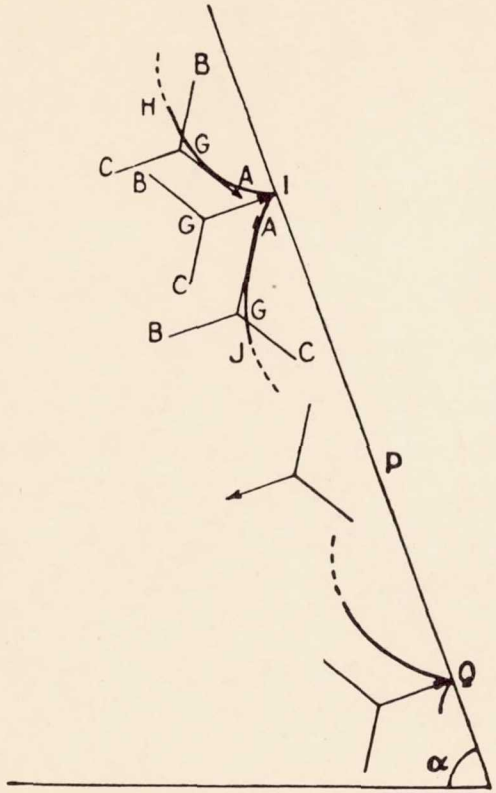

Figure 30.

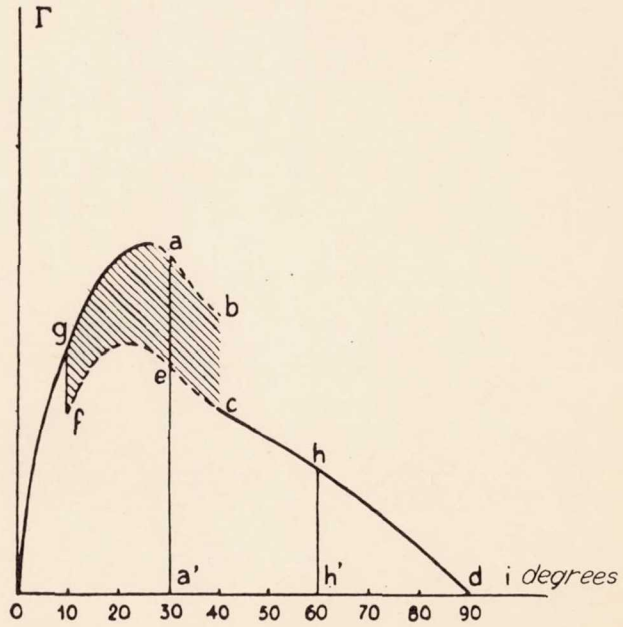

Figure 31.

Page intentionally left blank

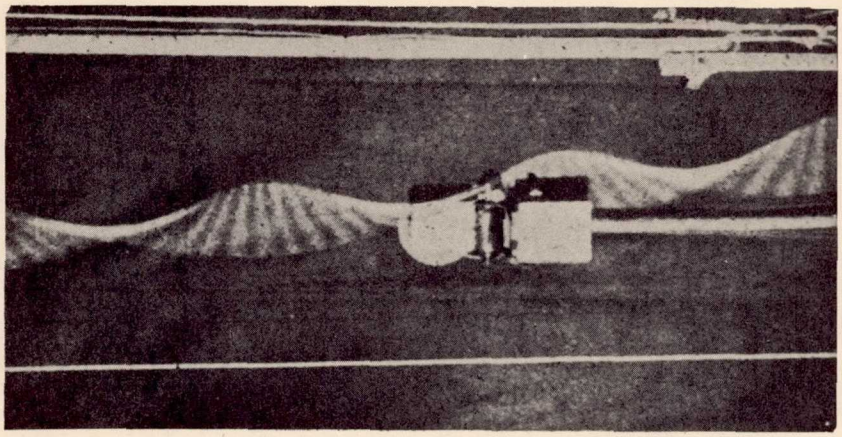

Figure 33.

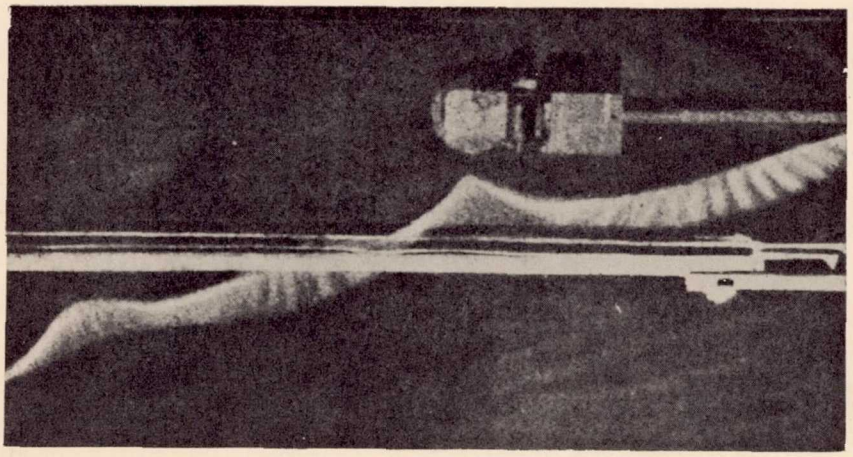

Figure 32.

Page intentionally left blank

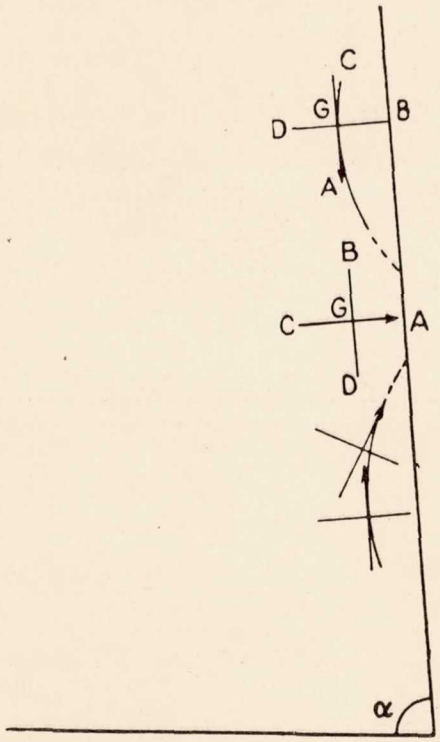

Figure 34.

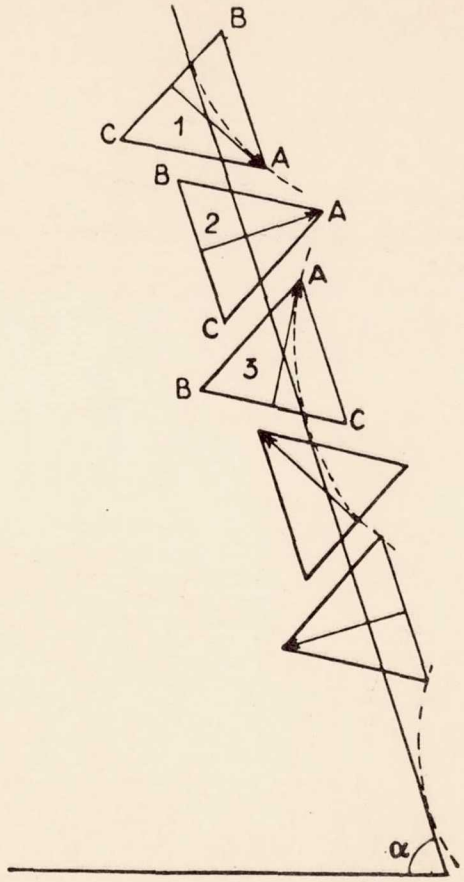

Figure 35.

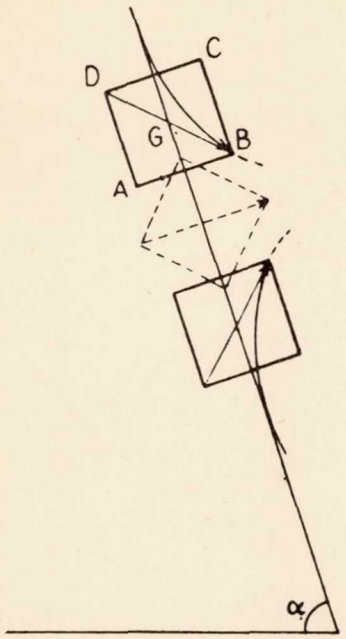

Figure 36.

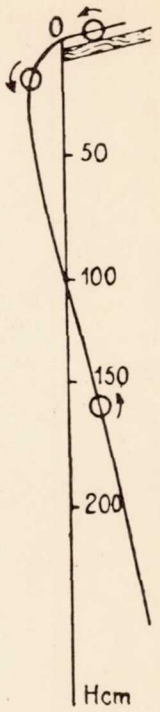

Figure 37.

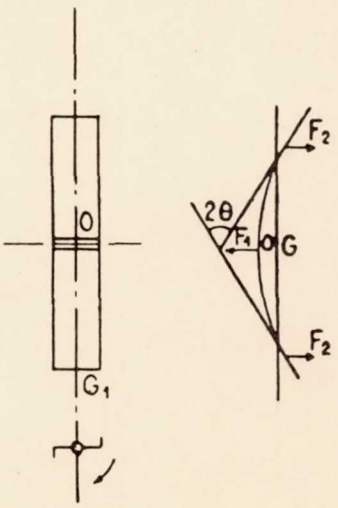

Figure 38.

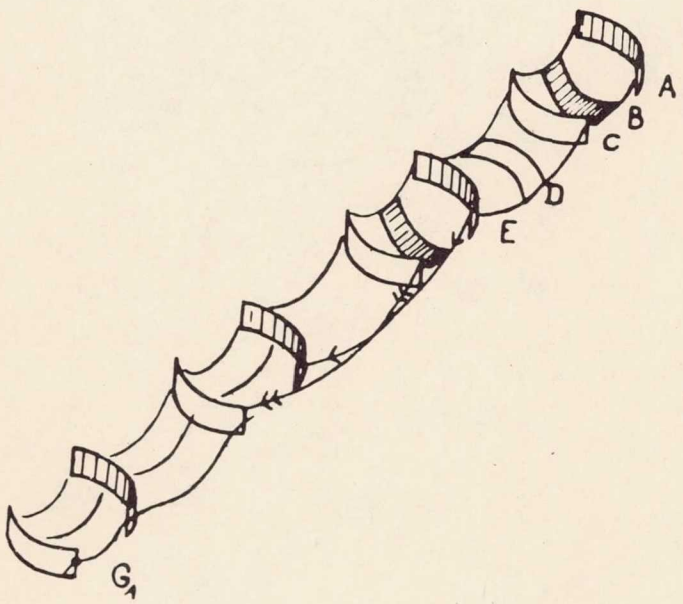

Figure 39.

Page intentionally left blank

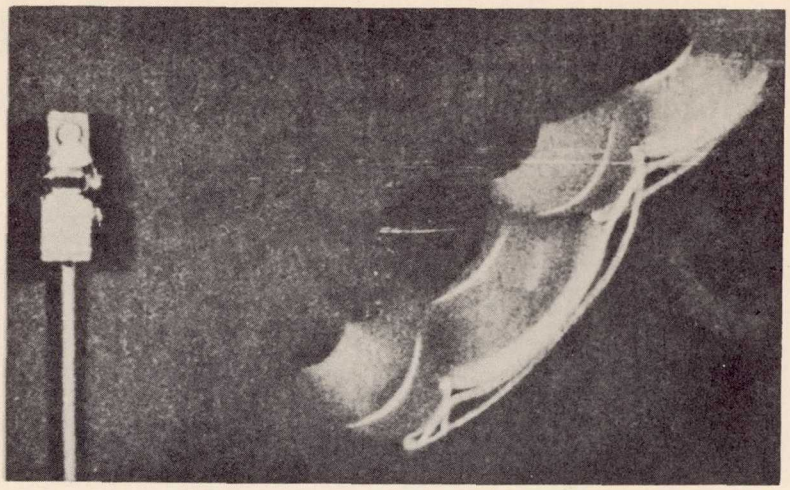

Figure 40.

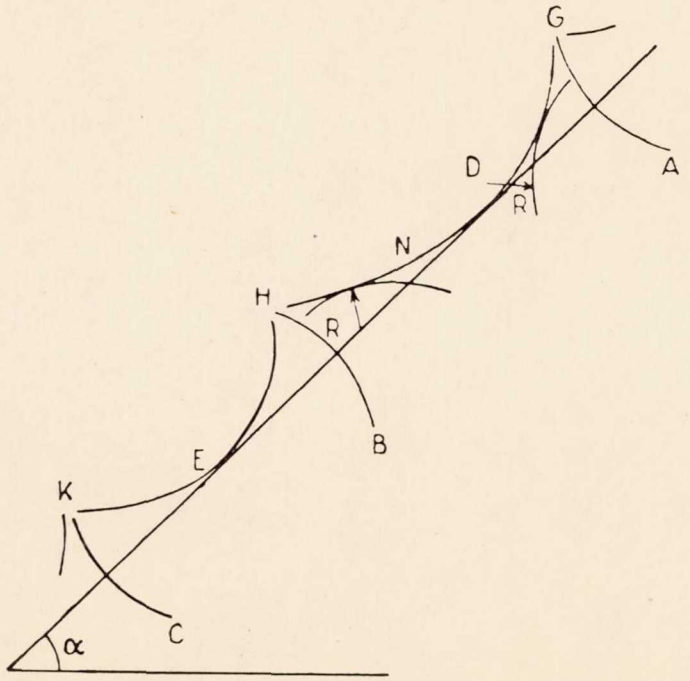

Figure 41.

Page intentionally left blank

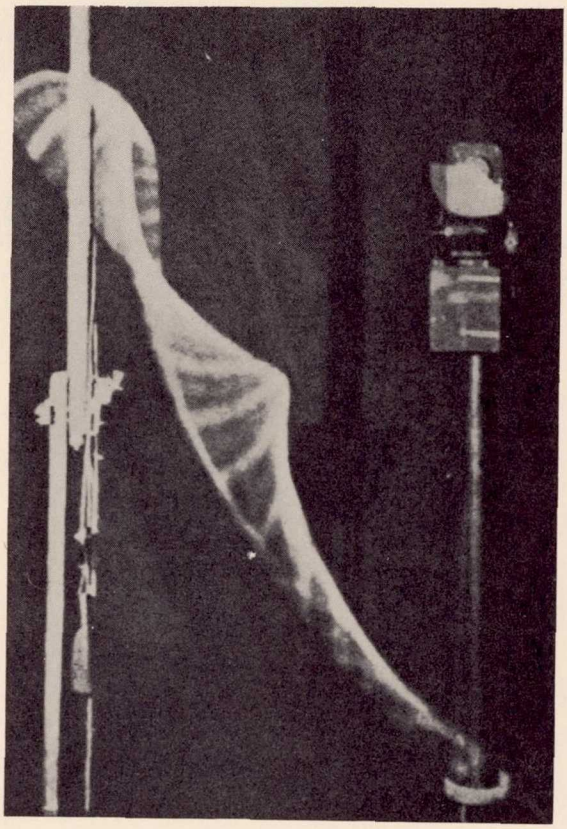

Figure 42.

Page intentionally left blank

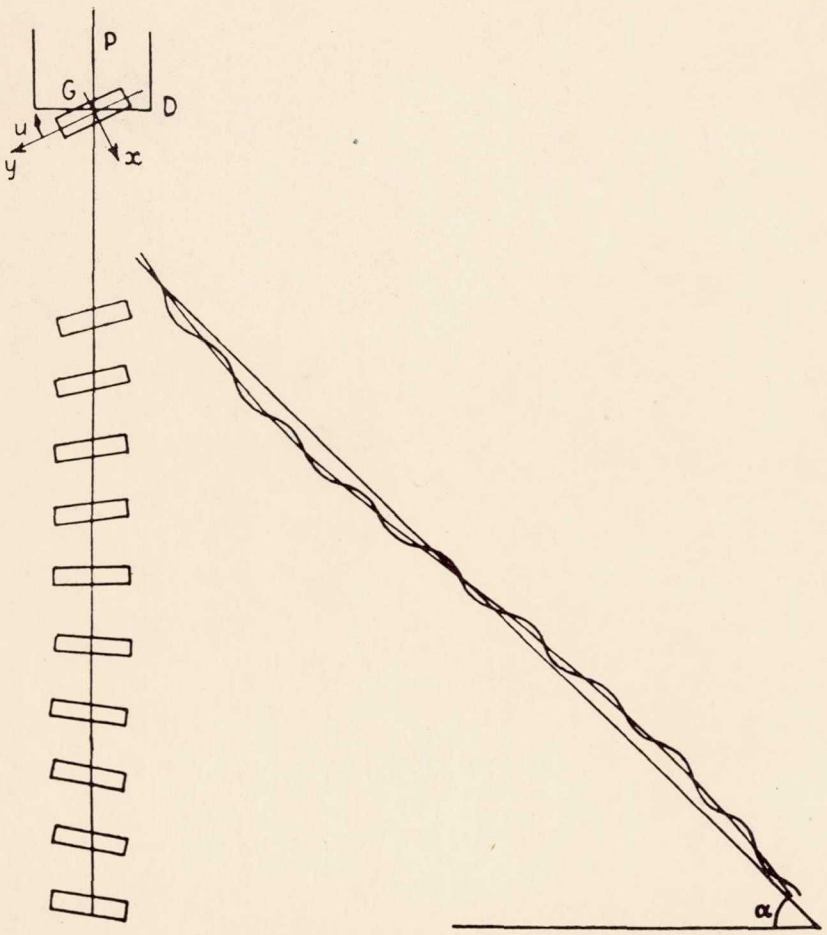

Figure 43.

Page intentionally left blank

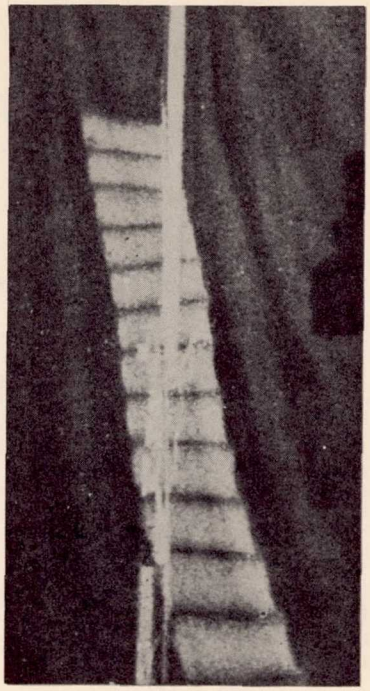

Figure 44.

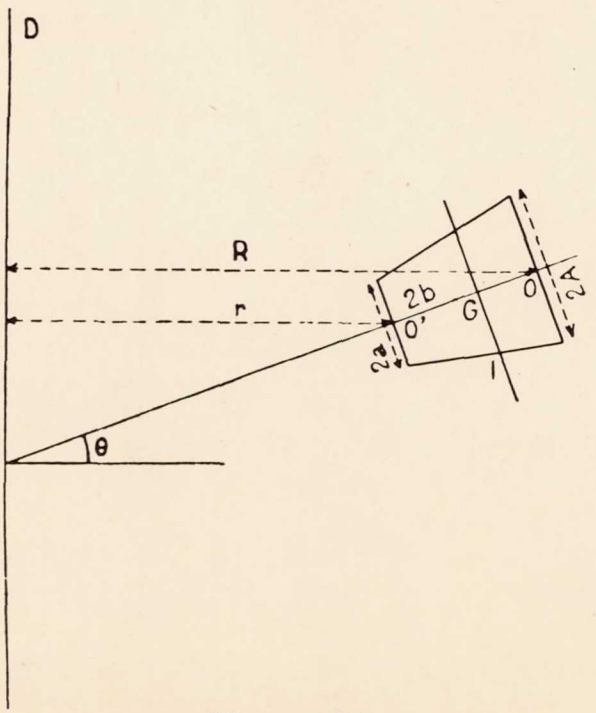

Figure 45.

Page intentionally left blank

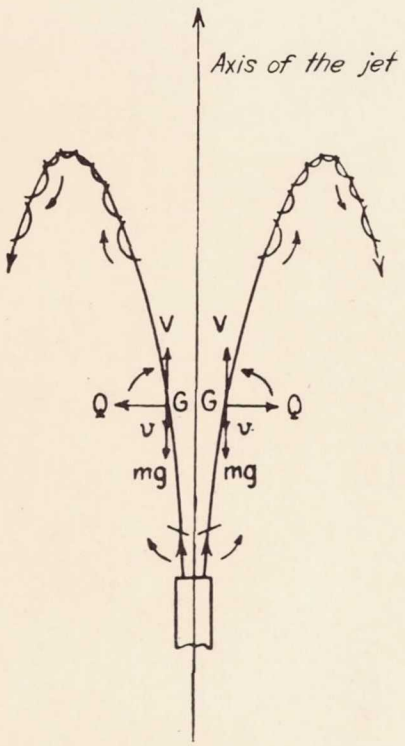

Figure 46.

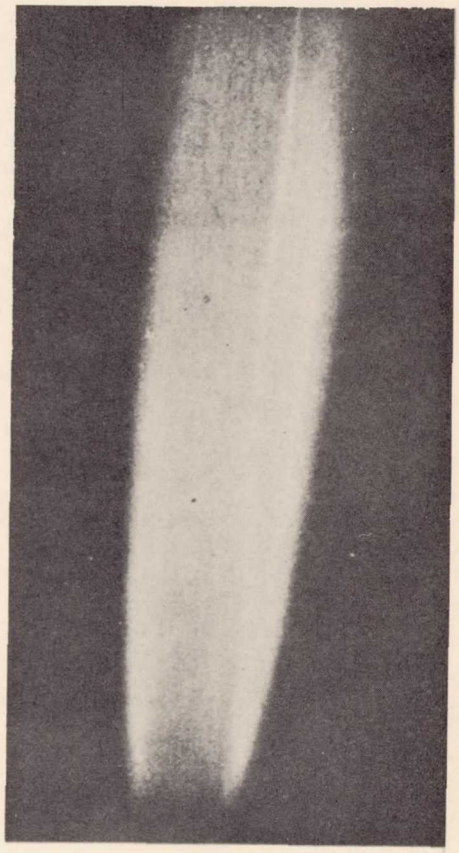

Figure 47.

Page intentionally left blank

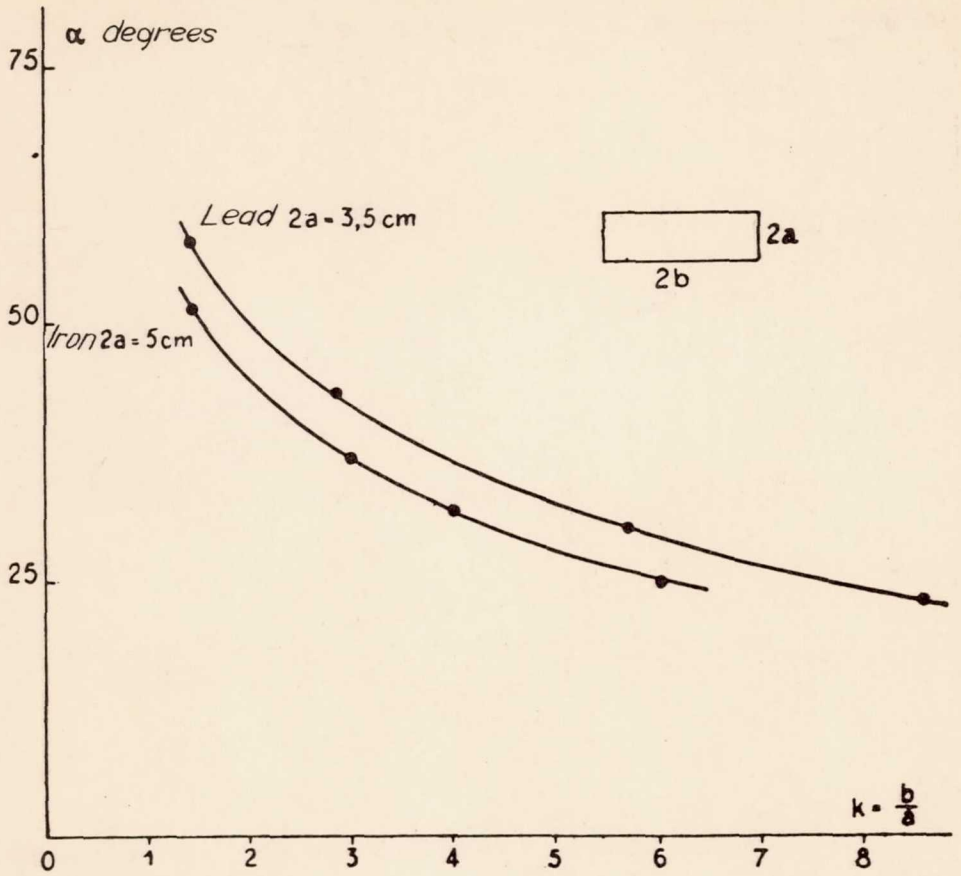

Figure 48.

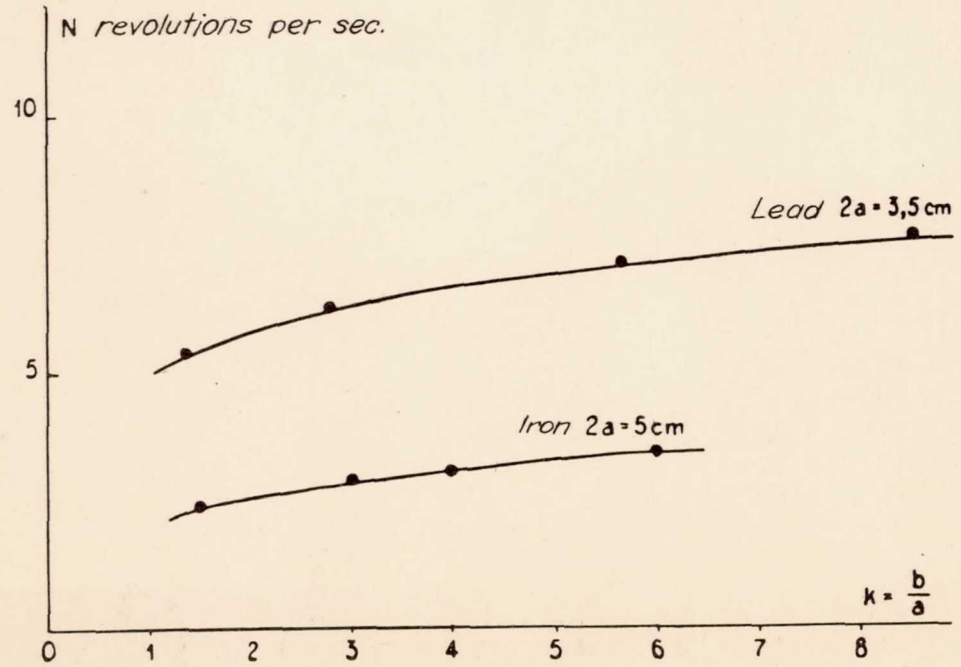

Figure 49.

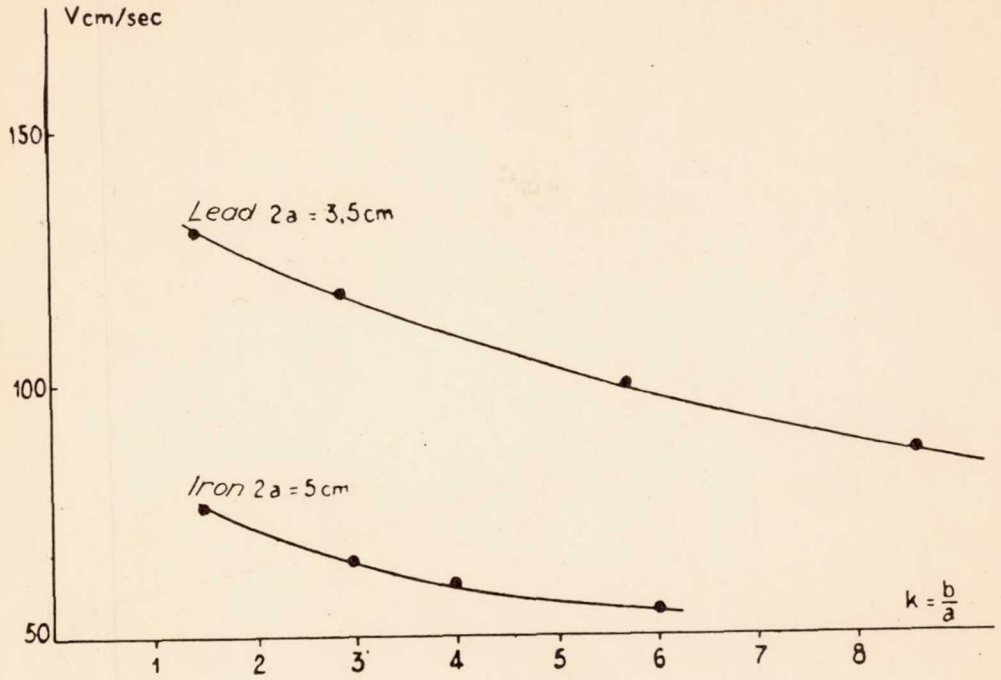

Figure 50.

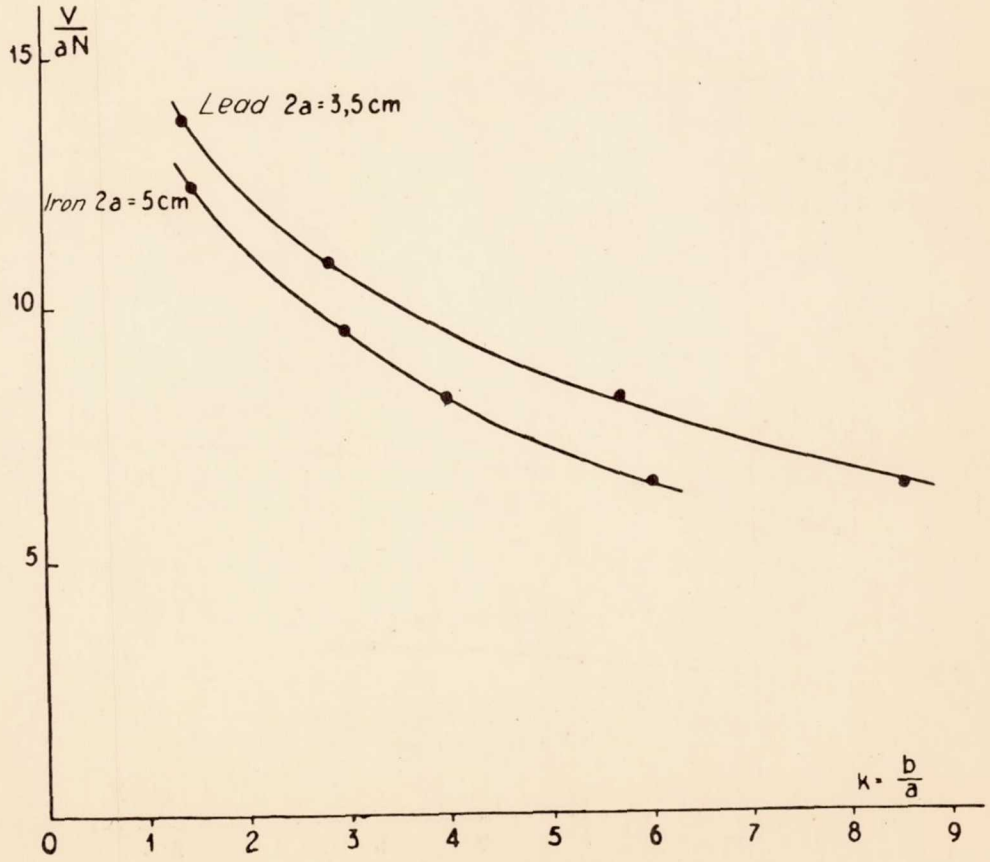

Figure 51.

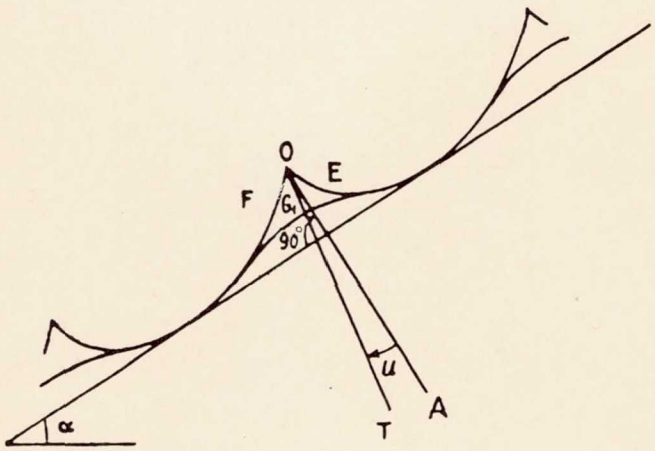

Figure 52.

Page intentionally left blank

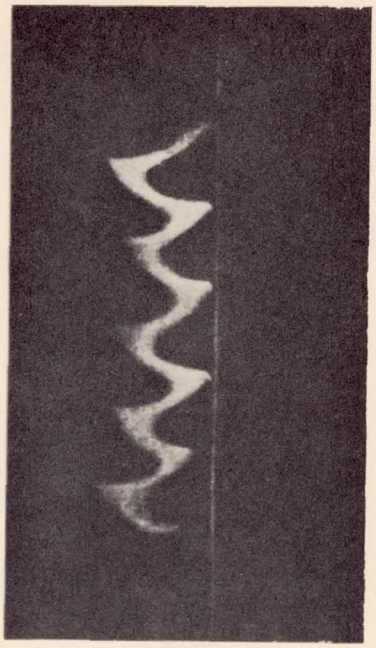

Figure 53.

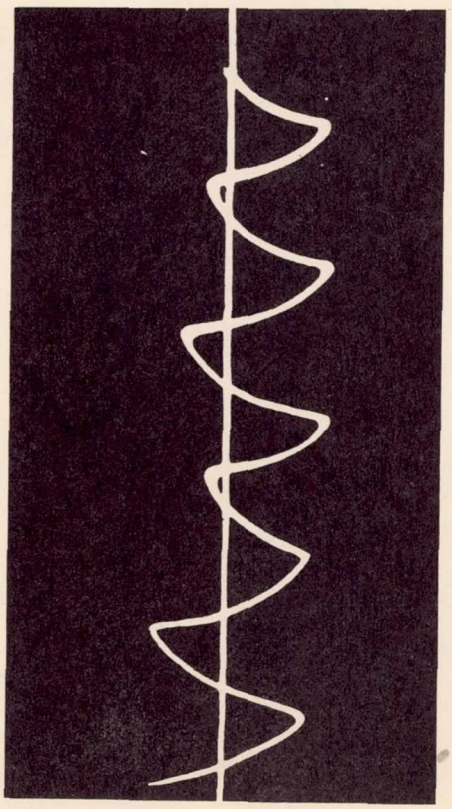

Figure 54.